49-я Школа ПИЯФ по Физике
Конденсированного Состояния
16-21 марта 2015, Санкт-Петербург
Зеленогорск

Вклад кристаллографии в разработку материалов для Li-аккумуляторов

Е.В. Антипов

Химический факультет МГУ имени М.В. Ломоносова

Outline

- Introduction
- Main types of cathode materials for LIB:

  Layered ($LiMO_2$) and $LiFePO_4$
- A_2MPO_4F fluoride-phosphates
- Concluding remarks

1995: «Advances in battery research are always restricted by chemistry »

R. E. Powers (N.Y. Times)

and Crystallography!

Energy storage systems

up to 250 Wh/kg

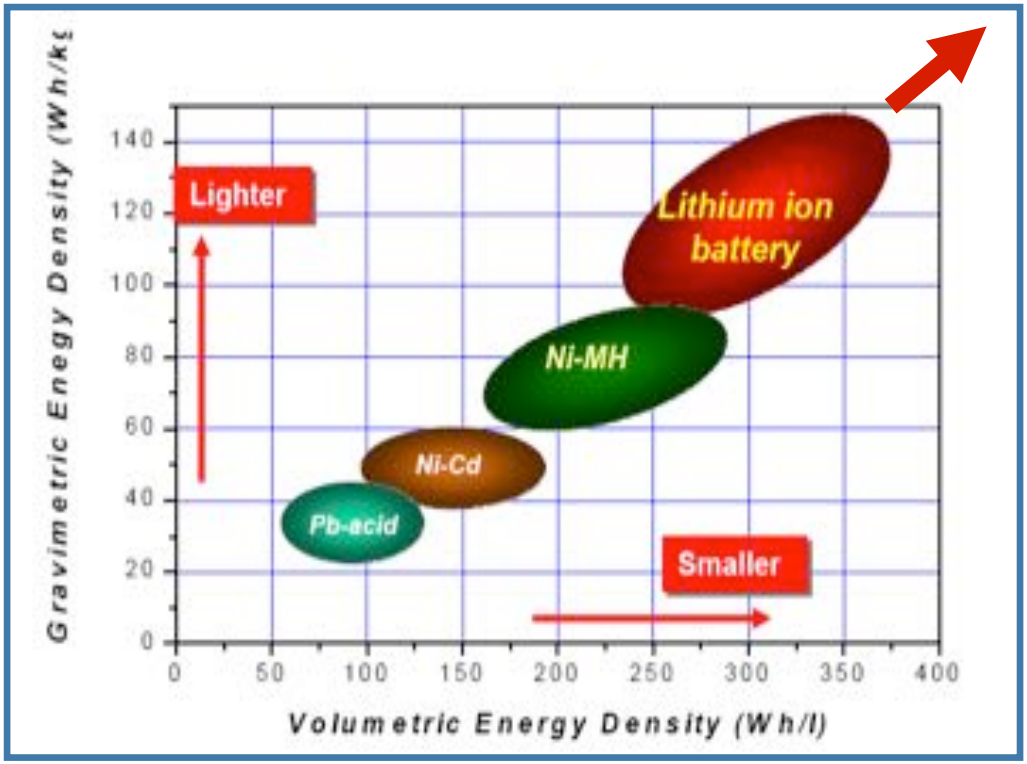

Stationary energy storage

HEV, EV

Consumer electronics

Increase of Energy and Power

Perspectives for Li-ion batteries

"Battery technology is one of the most important subjects affecting the technological future of man"

Charlie Munger
Vice Chairman of Berkshire

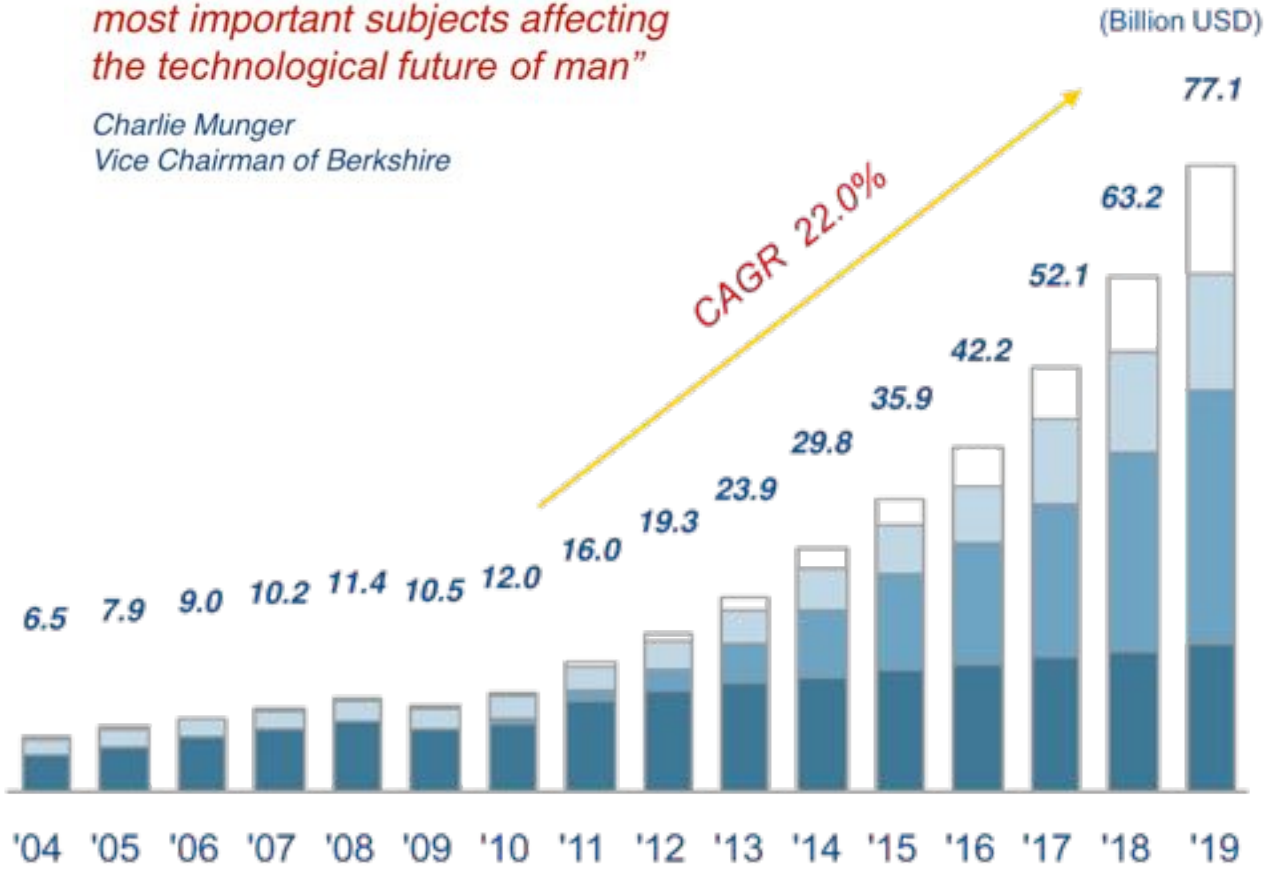

	Share ('19)	CAGR ('09-'19)
Robot	17.6%	52.4%
Storage	18.5%	18.2%
EV	40.5%	79.8%
IT	23.3%	9.1%

Yunil HWANG, A. D. Little Korea, Korea, "Nano-enhanced Market Perspectives in Solar & Li-ion Battery" OECD workshop on "Nanotechnology for sustainable energy options", 2010

Development of Electric Vehicles

La Jamais Contente - 1899

- 2 electric motors with 50 kW in total
- 200 individual Pb-PbO_2 cells
- **Total mass 1450 kg**
- Battery mass > 700 kg
- Max. speed 106 km/h

Nissan leaf - 2010

Total weight	1500 kg
Batteries weight	**300 kg**
Stored Energy	**24 kWh**
Power	120 h.p.
Distance	**70 – 220 (150) km**
Maximum speed	150 km/h

Cathode material – $LiMn_2O_4$
(E_g = 80 Wh/kg)

Safety problem

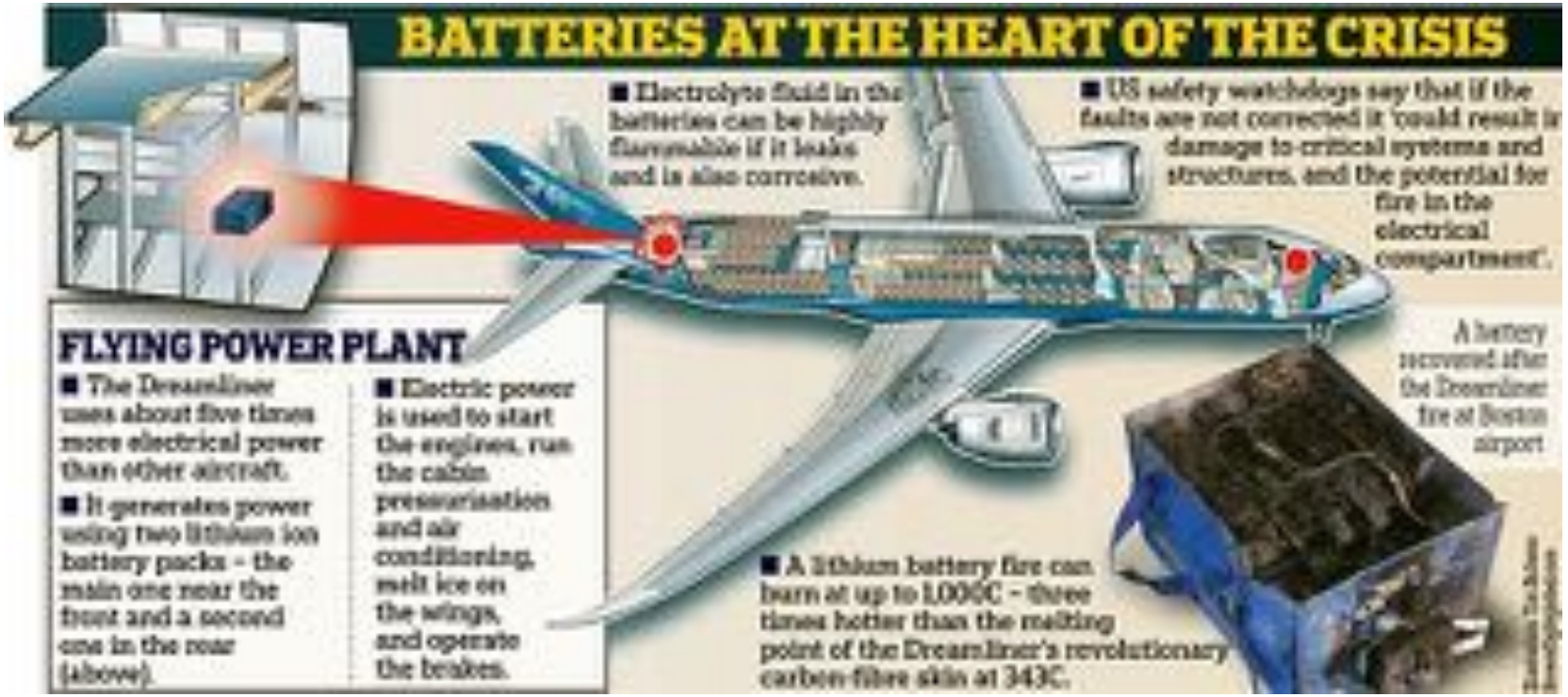

Daily Mail, 20.01.2013

Impact of crystallography

Design of new structures:
- crystal chemistry concepts
- data mining
- *ab initio* structure predictions

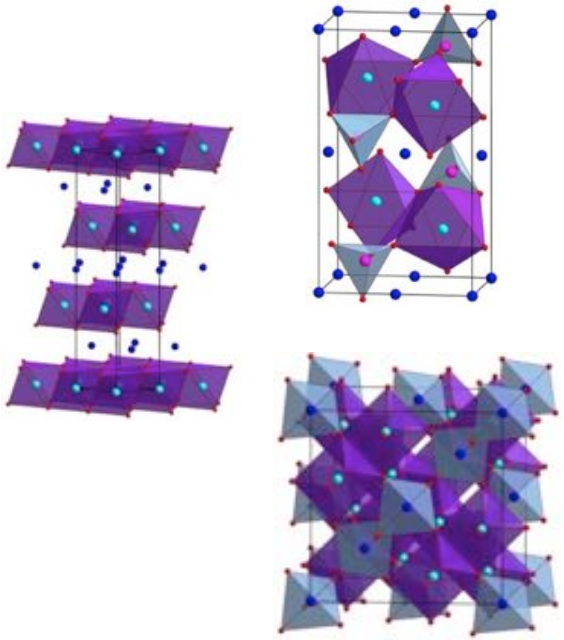

Crystallographic aspects of electrochemical reactions:
- *in situ* and *ex situ* X-ray and neutron diffraction studies
- spectroscopic methods (EXAFS, XPS, XANES etc)
- microstructure evolution

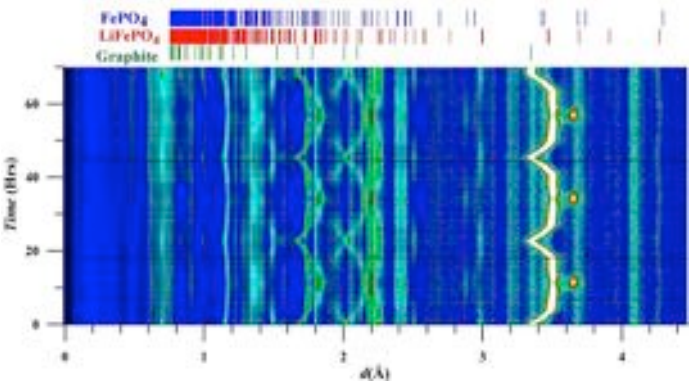

I.A. Bobrikov et al. ,
J. Power Soc.. 258 (2014) 356

Electrochemical processes on atomic scale:
- *ex situ* electron diffraction (PED) studies, atomic resolution TEM imaging and spectroscopy
- *in situ* TEM

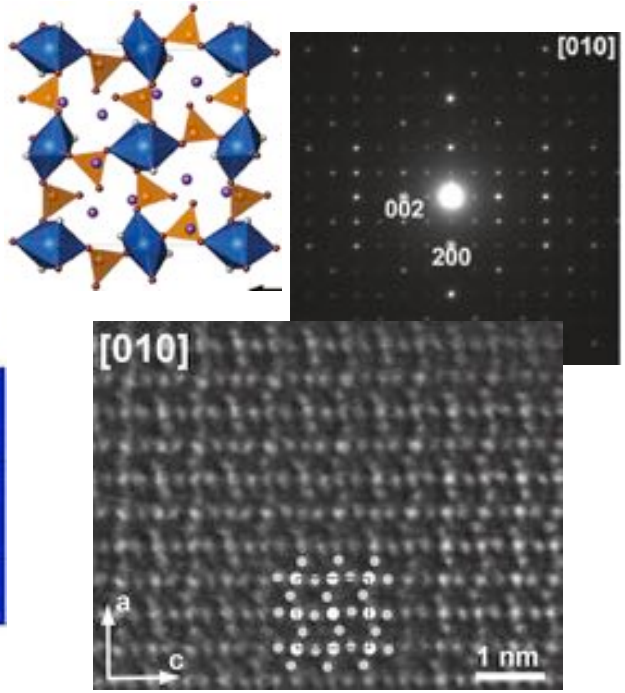

J. Hadermann et al. ,
Chem. Mat. 23 (2011) 3540

Main discovery

Mat. Res. Bull., Vol. 15, pp. 783-789, 1980. Printed in the USA.
0025-5408/80/060783-07$02.00/0 Copyright (c) 1980 Pergamon Press Ltd.

Li_xCoO_2 ($0<x\leq1$): A NEW CATHODE MATERIAL FOR BATTERIES OF HIGH energy DENSITY

K. Mizushima, P.C. Jones, P.J. Wiseman and J.B. Goodenough
Inorganic Chemistry Laboratory, South Parks Road, Oxford, OX1 3QR

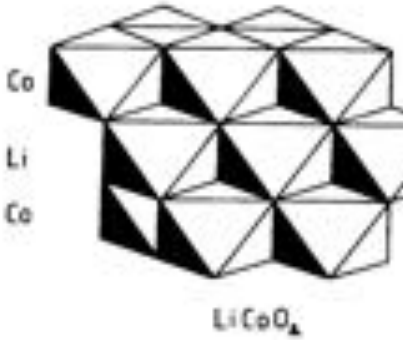

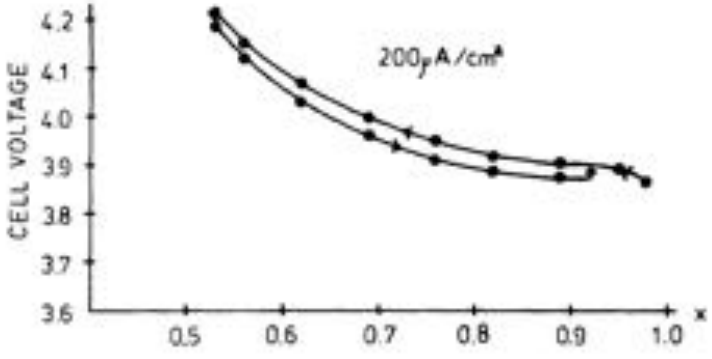

Examination of the known Li^+-ion solid electrolytes led us to conclude that Li^+ ions may be mobile in close-packed oxygen arrays. Given that hypothesis, it was then natural to consider the transition-metal lithium oxides $LiMO_2$ crystallizing in the layered structure

Li-ion battery

Concept (1980) Commersialization: Sony (1990)

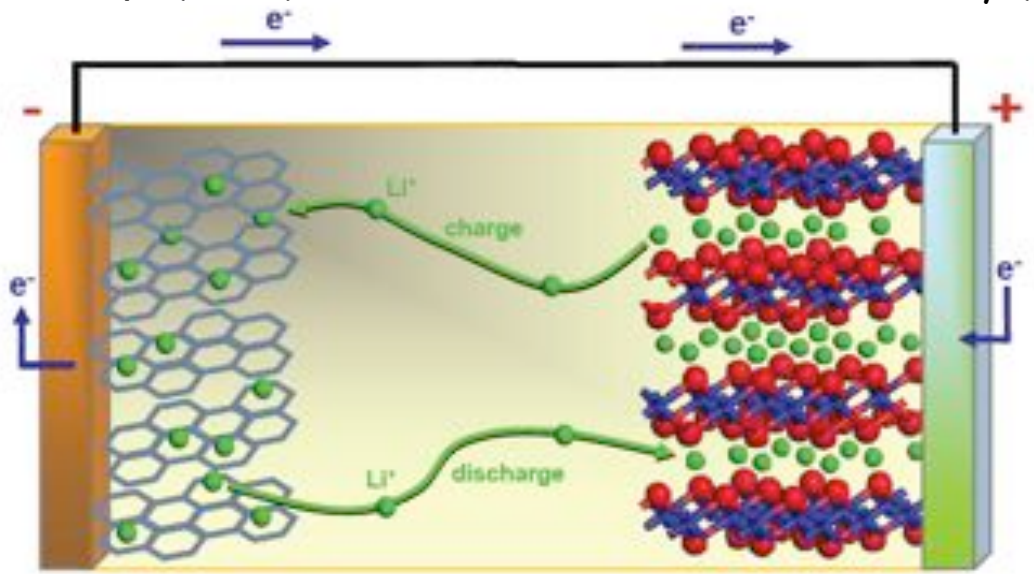

LixC6 graphite Li+- conducting electrolyte LiMO2

$$C_6 + LiCoO_2 \underset{discharge}{\overset{charge}{\rightleftharpoons}} Li_xC_6 + Li_{1-x}CoO_2 \qquad x \approx 0.5\text{-}0.6\ e^-$$

Voltage: 3.6 V **E^o (cathodic) – E^o (anodic) = E^o (cell)**

Electrolyte - salts: $LiPF_6$, $LiBF_4$ ($LiClO_4$, $LiAsF_6$), $LiCF_3SO_3$
- solvents: EC, PC, DMC, DEC **1M $LiPF_6$ in EC/DEC/DMC**

E_g(gravimetric) = **C_g** (charge transferred between two electrodes per unit weight) x **E^0** (cell)

Why Li ?

J.Goodenough & Y.Kim, Chem.Mat. 22 (2010) 587

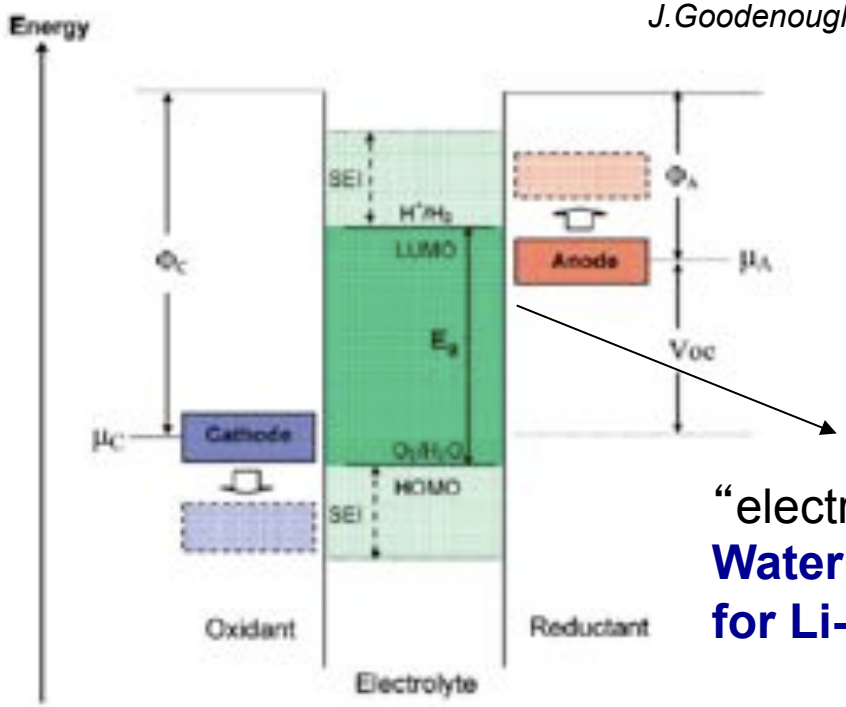

"electrolyte window"
Water – 1.23 V,
for Li-electrolytes – up to 4 V

1) Larger "electrolyte window" → **higher specific energy**

2) Weak Li-O bonds → **high Li-ion conductivity**

3) Low size → **mechanical stability**

Selection of Electrode Material

J.Goodenough & Y.Kim, Chem.Mat. 22 (2010) 587

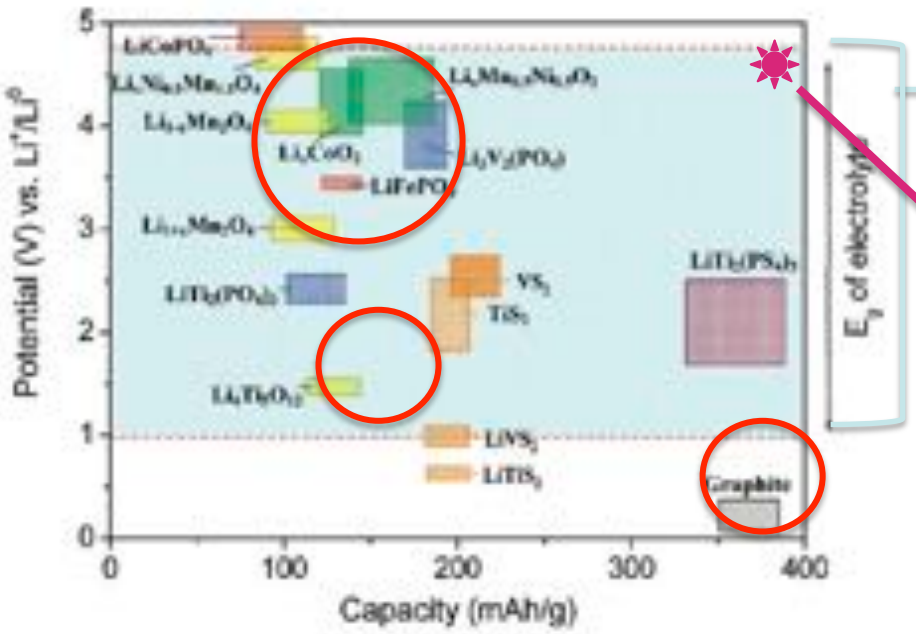

H_2O – 1.23 V,
Li-electrolyte – up to 4 V

Electrolyte window

(Oxidation and reduction of electrolyte outside the window)

How to reach this value?

To increase specific energy → to higher cathode potential and capacity

To increase power → to higher Li-ion diffusion rate

Cathode materials: characteristics and requirements

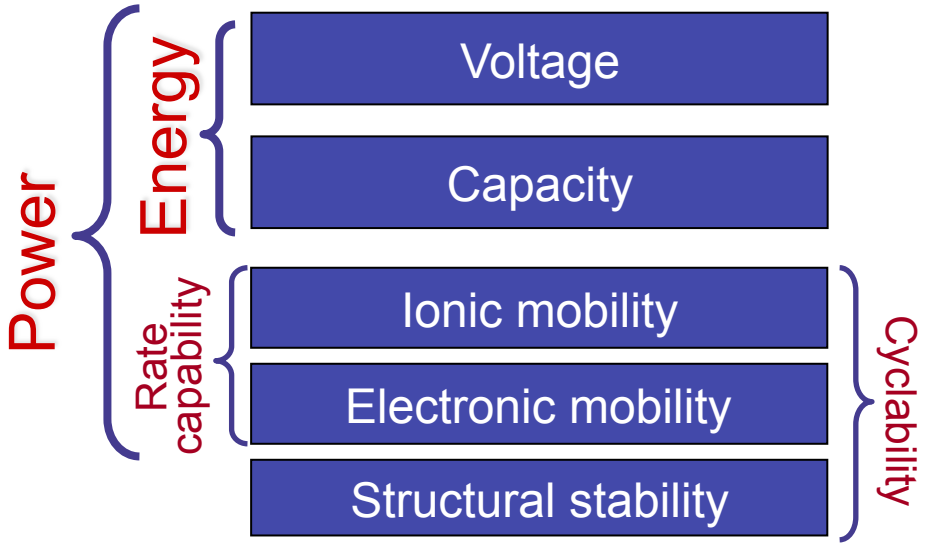

$M^{n+}/M^{(n+1)+}$ redox potential

$$C_T\,(A\,h\,g^{-1}) = \frac{26.8 \times \Delta n}{M}$$

Δn: number of e^- or Li^+

M: Molecular weight (g)

Energy = Voltage x Capacity

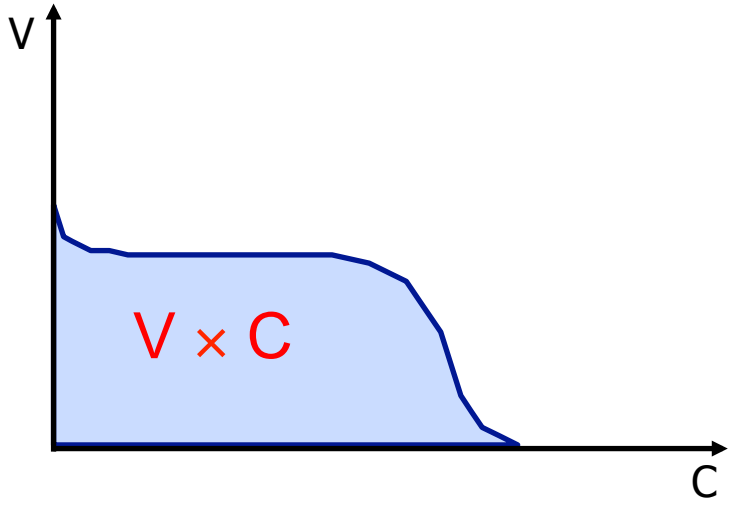

Cathode materials: characteristics and requirements

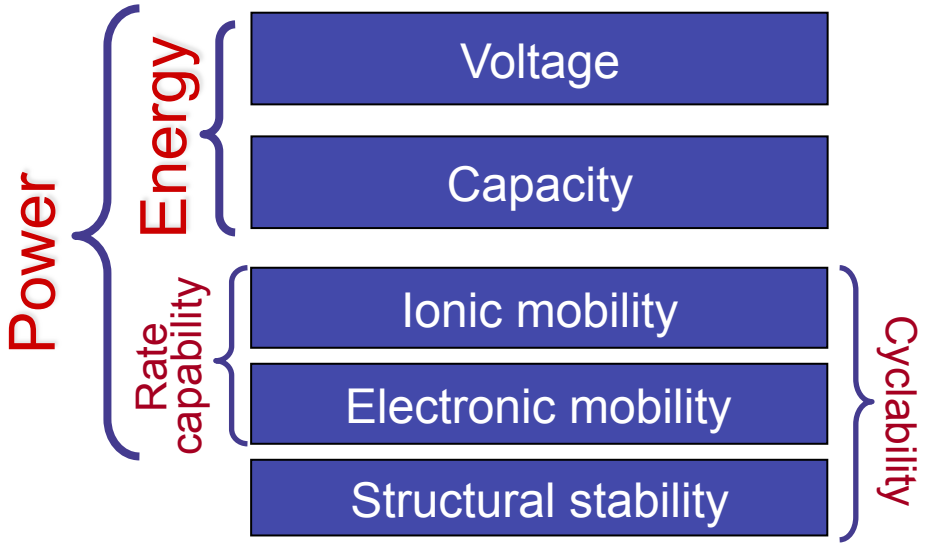

$M^{n+}/M^{(n+1)+}$ redox potential

$$C_T\,(A\,h\,g^{-1}) = \frac{26.8 \times \Delta n}{M}$$

Δn: number of e^- or Li^+

M: Molecular weight (g)

Energy = Voltage x Capacity

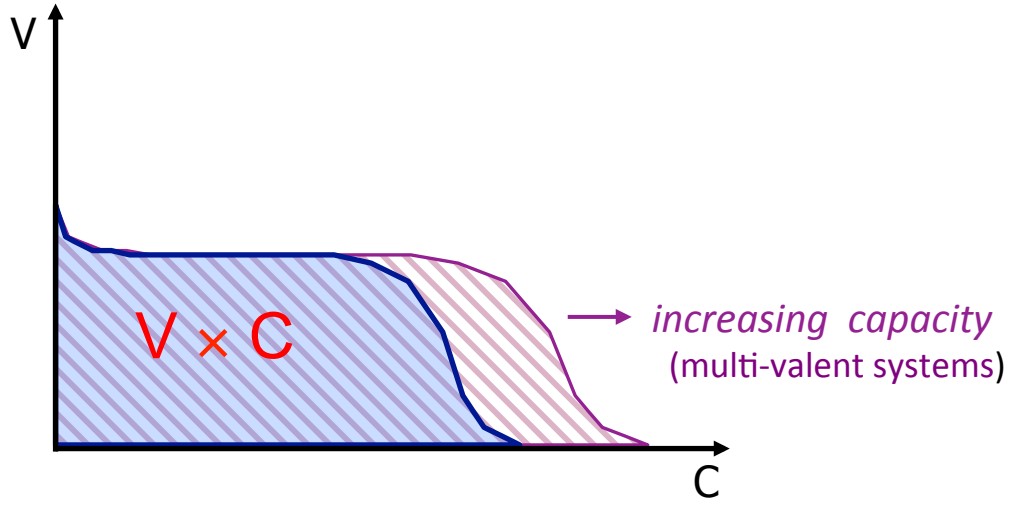

Cathode materials: characteristics and requirements

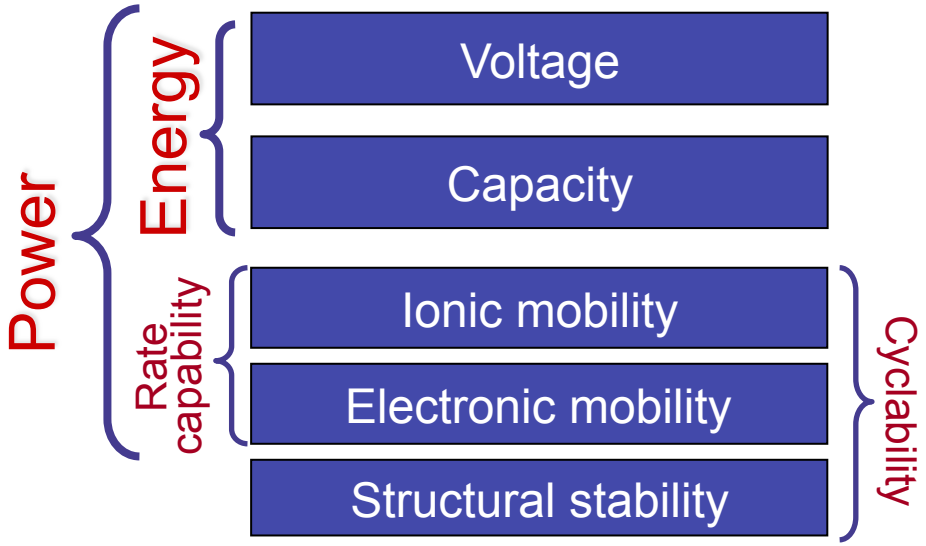

$M^{n+}/M^{(n+1)+}$ redox potential

$$C_T\,(A\,h\,g^{-1}) = \frac{26.8 \times \Delta n}{M}$$

Δn: number of e^- or Li^+

M: Molecular weight (g)

Energy = Voltage x Capacity

≤ 4.8 V (vs. Li/Li^+)

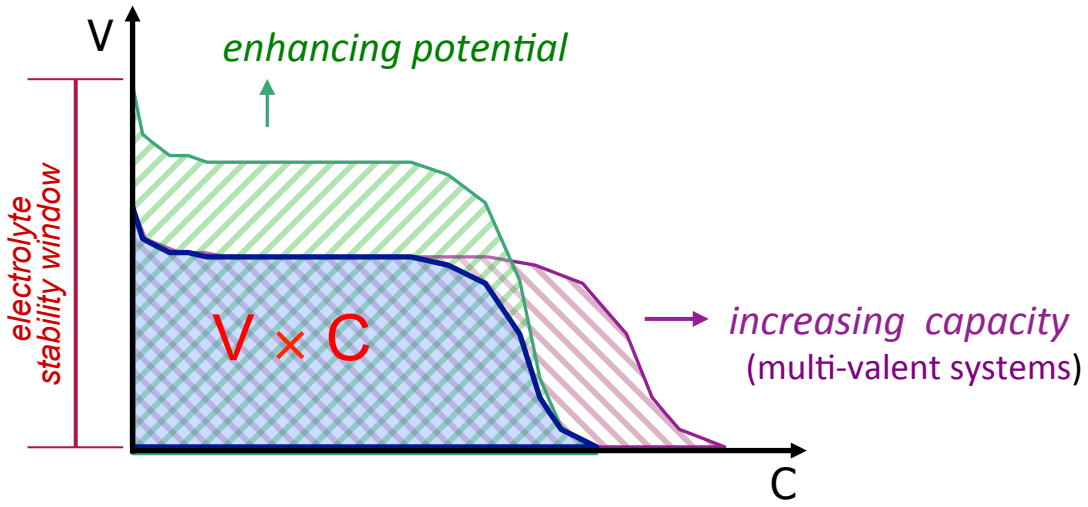

Selection of composition

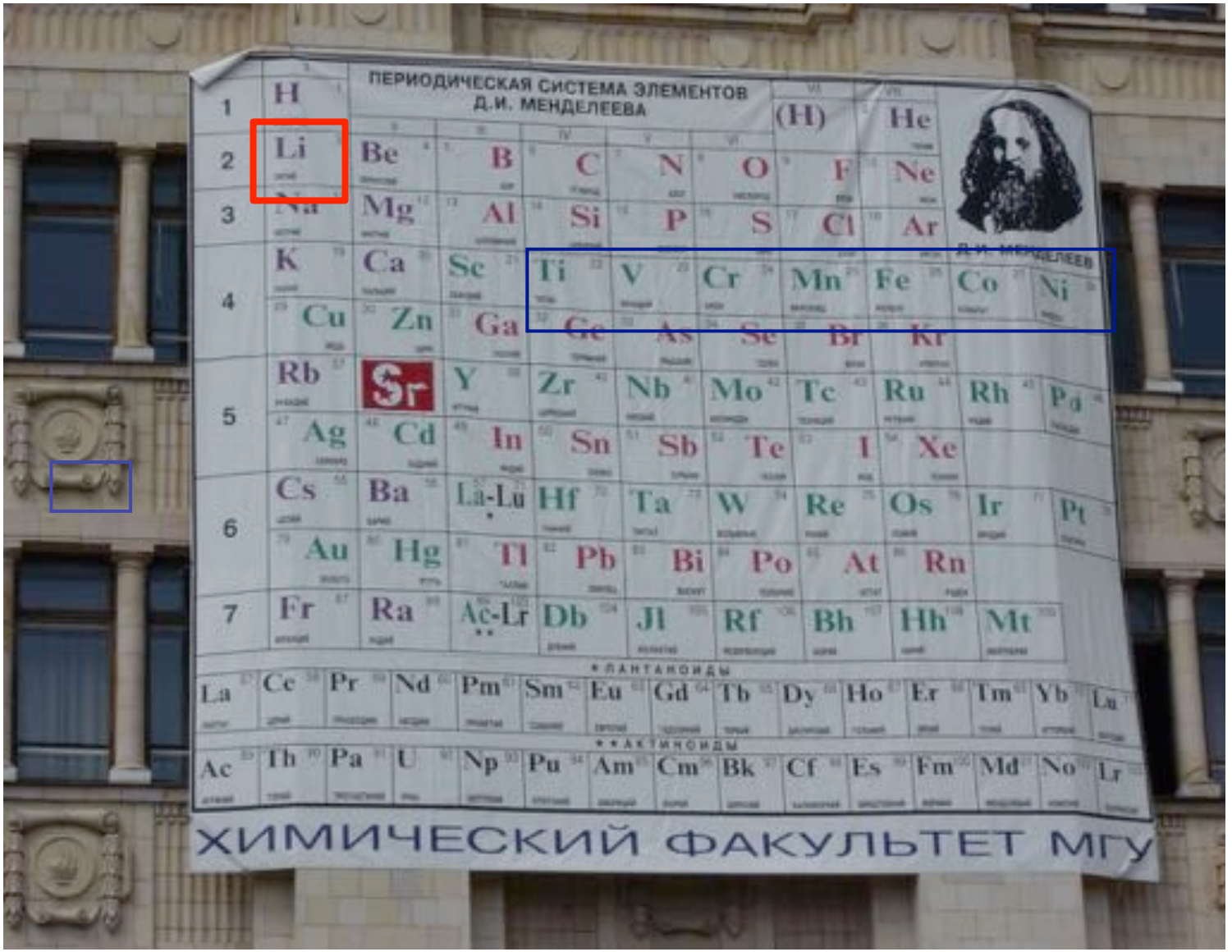

Main Structure Types

$LiCoO_2$

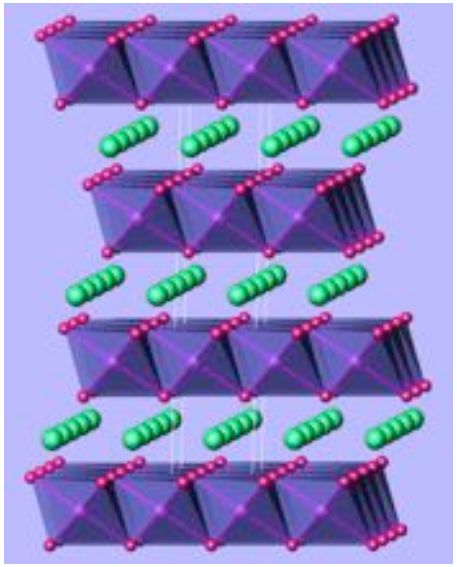

$LiMn_2O_4$

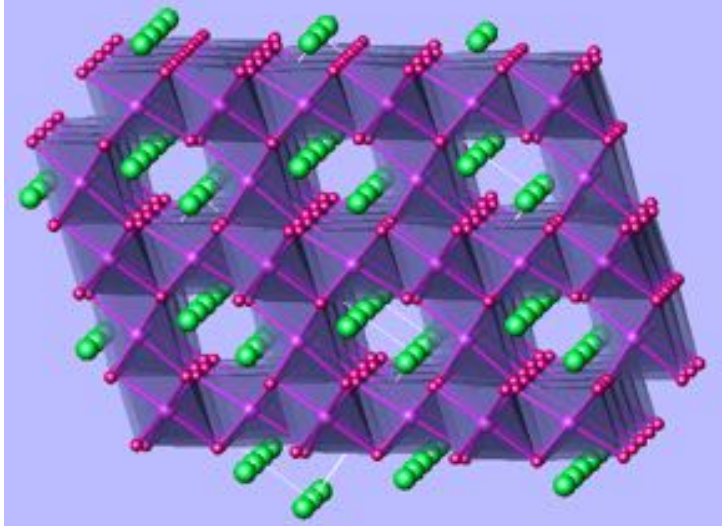

$LiFePO_4$

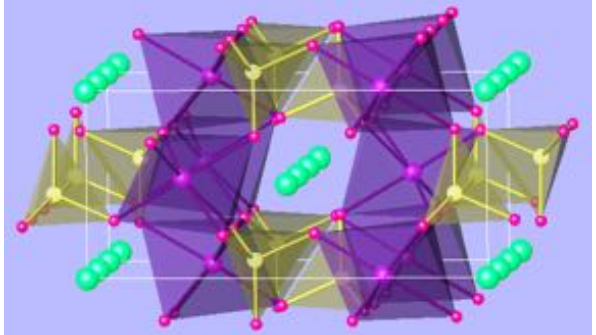

Hexagonal close packing

Cubic close packing

C_t	278 mAh/g ($0.5C_t$)	148 mAh/g	170 mAh/g
E_g	556 Wh/kg	592 Wh/kg	583 Wh/kg
σ	10^{-3} S/cm	10^{-5} S/cm	10^{-9} S/cm
D	10^{-9} cm^2/s	10^{-10} cm^2/s	10^{-15} cm^2/s

Layered $LiMO_2$ oxides

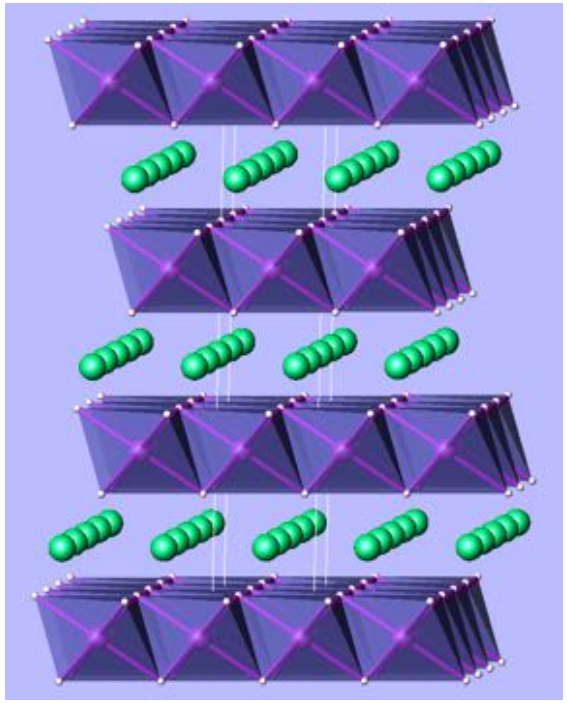

α-$NaFeO_2$

$LiMO_2$ (M = Fe, Mn, Co, Ni)

Li^+ - 0.74 Å

	Mn^{3+}	Fe^{3+}	Co^{3+}	Ni^{3+}
RVI, Å	0.58 (LS) 0.65 (HS)	0.55(LS) 0.65(HS)	0.525(LS) 0.61(HS)	0.56(LS) 0.60(HS)

Co^{3+} LS ($t_{2g}^6 e_g^0$) ⟷ HS ($t_{2g}^4 e_g^2$)

	Fe	Mn	Ni	Co
Market price of metal [$/kg]	0.23	0.5	13	25
Atomic contents in crust [ppm]	50000	950	75	25
Permissible amount in air [mg/m^3]	10	5	1	0.1
Permissible amount in water [mg/L]	300	200	13.4	0.7

Problems:

Cation disorder

Stability (oxygen evolution, structure transformation)

Cost

Ecology

Influence of cation disorder

Suppression of cation disorder: synthesis by cation exchange from $NaNi_{0.5}Mn_{0.5}O_2$

$\Delta c = 0.06$ Å

Li-slab 2.59 Å (SS) and 2.65 Å (IE)

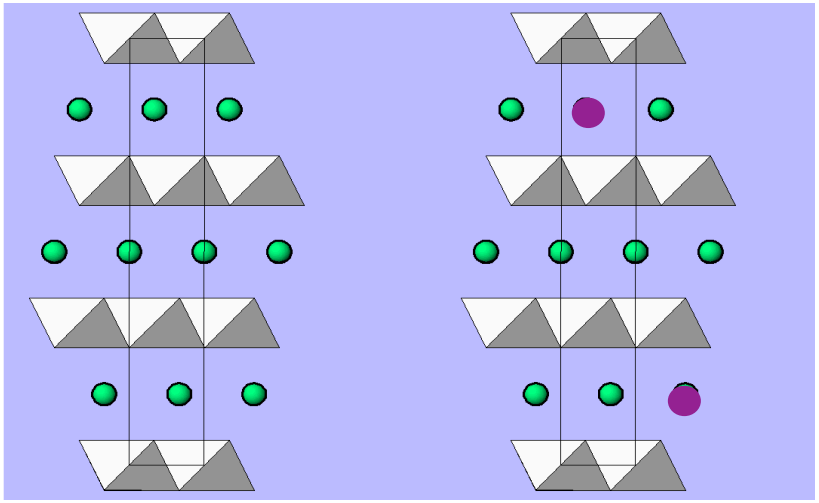

α-$NaFeO_2$ $Li_{1-y}N_{i1+y}O_2$

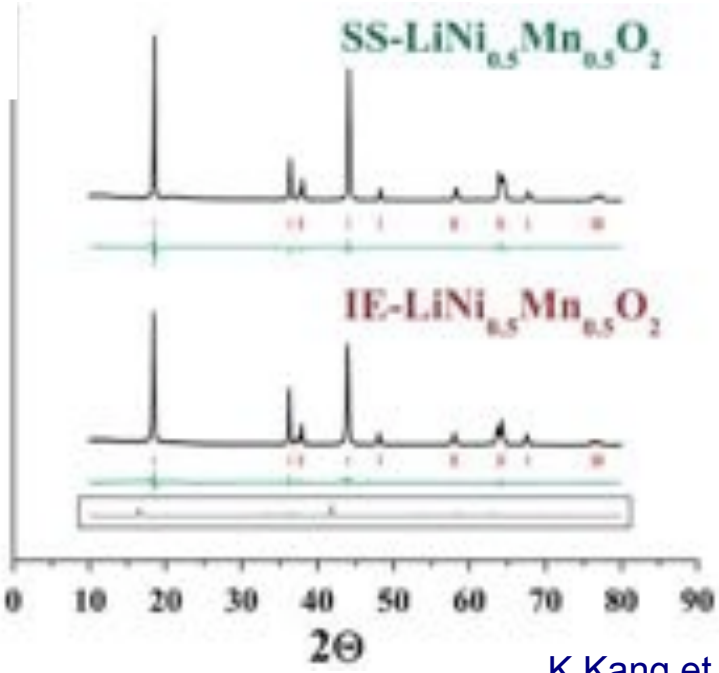

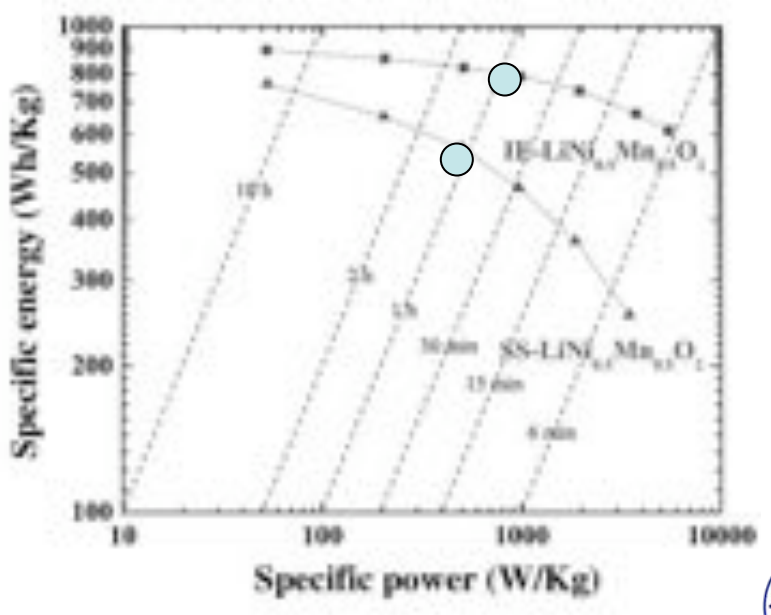

K.Kang et al. Science 311 (2006) 977

$LiFePO_4$ - olivine

c_t = 170 mAh/g; E ~ 3.5 V

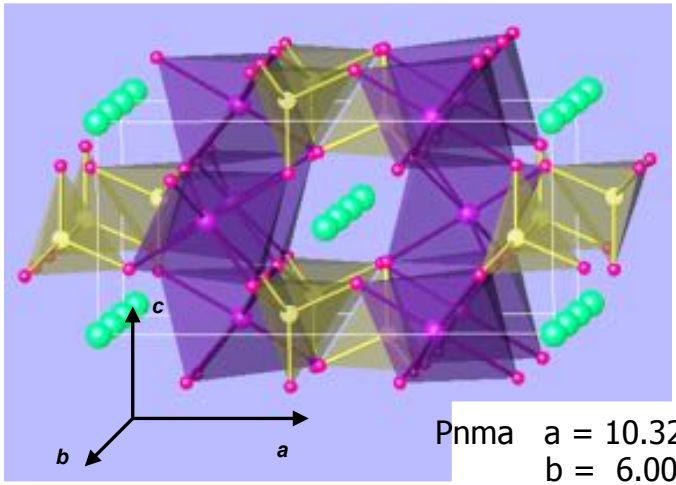

Pnma a = 10.3223(15)Å
b = 6.0047(9) Å
c = 4.6929(7) Å

Advantages:

- stable material (3D structure + PO_4)
  $LiFePO_4$ ⇐⇒ $FePO_4$ + Li^+ + e-
- ecologically friendly
- cheap

Disadvantages:

- low electronic conductivity~ 10^{-9} S/см
- low D~10^{-15} cm^2/s ($t \approx r^2/D$)/
  2-phase mechanism
- low density
- medium potential
  (for phases with Mn = 4.2 V, Co = 4.9 V)

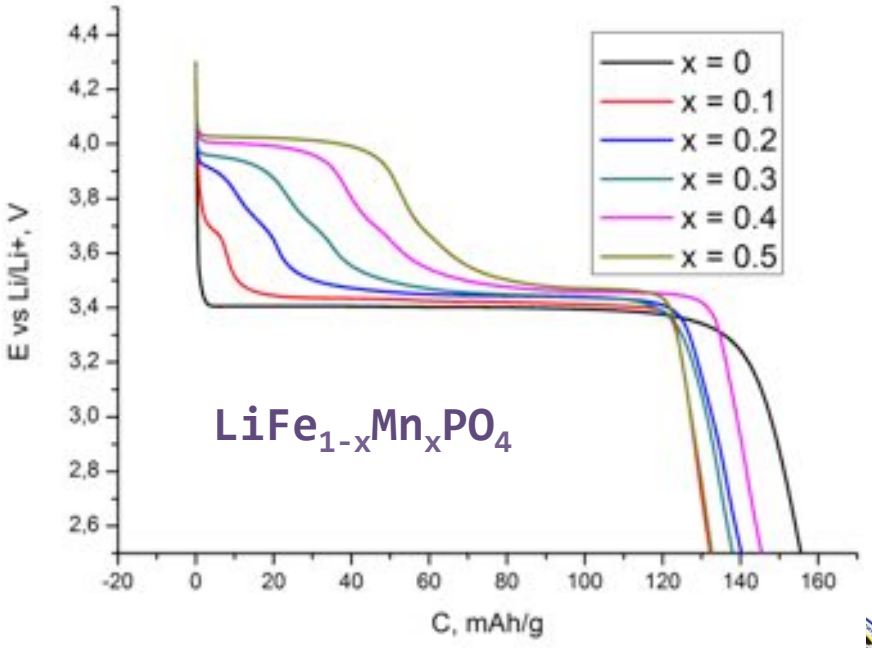

A. K. Padhi, et al., *J. Electrochem. Soc.* 144 (1997) 1609

Li-ion diffusion pathway

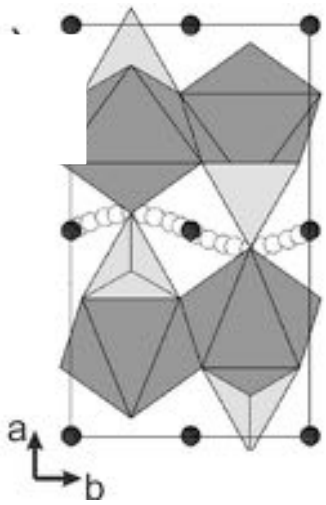

MD *(M.S. Islam et al. Chem. Mater. 17 (2005) 5085*

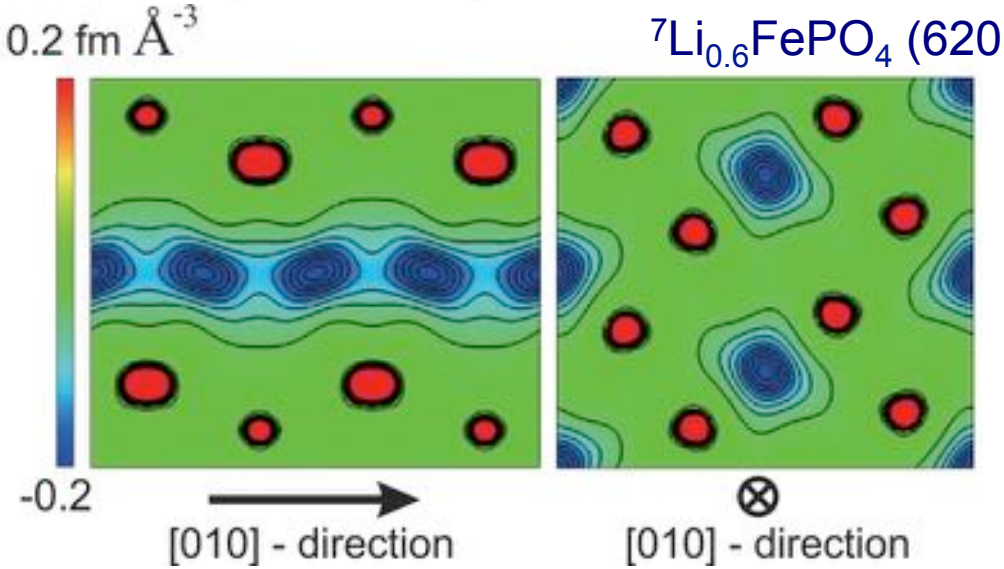

NPD/MEM*: S.I. Nishimura et al. Nature Materials 7 (2008) 707*

BVS mapping with 3DBVSMAPPER program

$$BVS = \sum_{j=1}^{N}\left[\exp\left(\frac{R_o - d_j}{b}\right)\right]$$

d_j - bond distance,
Ro, b – tabular constants

M. Sale, M. Avdeev, *J. Appl. Cryst*. 45(2012),1054

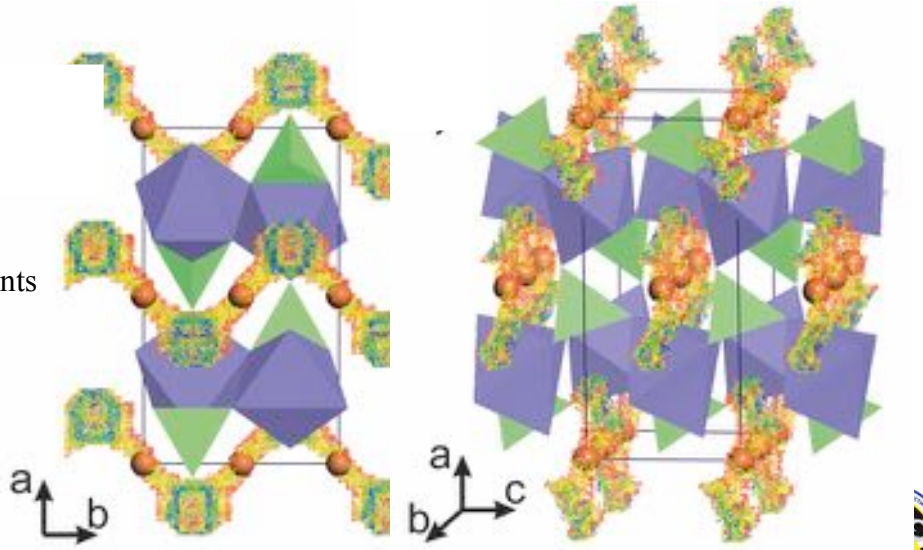

$LiFePO_4$: transport properties improvement

Carbon coating

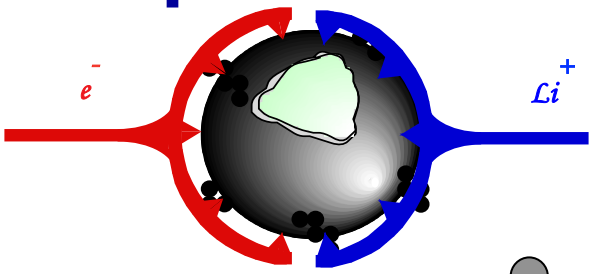

Nano-structuring

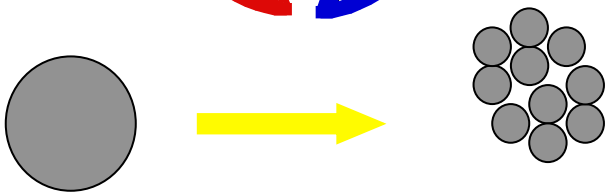

Nano

Morphology optimization

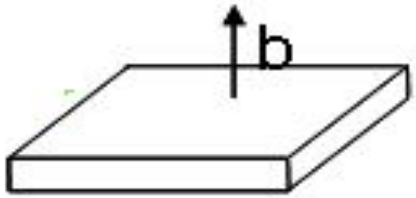

Platelet-type particles

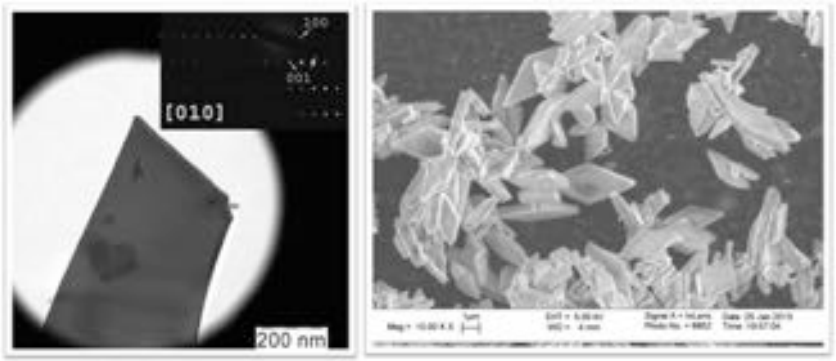

HT-synthesis

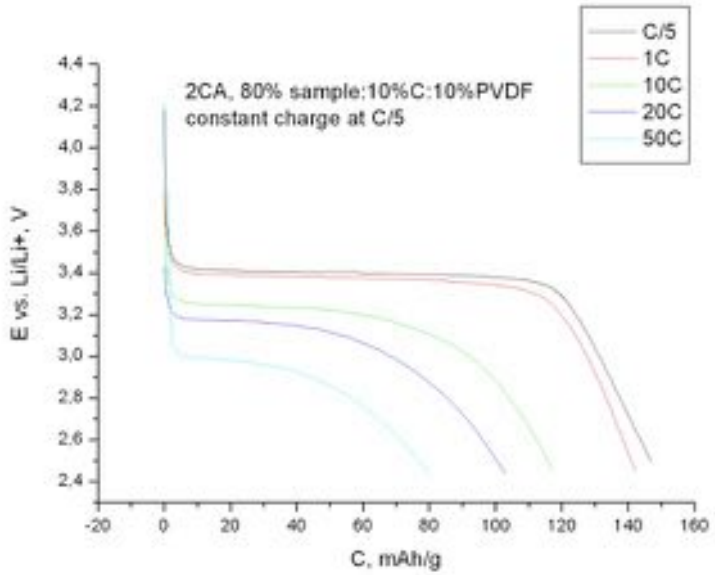

Bond valence summation (BVS)

2nd Pauling rule:
bond valence sum of cations converging on an anion should be equal to the valence of the anion

D. Altermatt, I. D. Brown (1985)

$$BVS = \sum_{j=1}^{N} \left[\exp\left(\frac{R_o - d_j}{b} \right) \right]$$

dj - bond length,
*R*o, *b* – tabular constants

Bond valence sum = formal oxidation state of the anion

Altermatt, Brown, Brese, O'Keefe – analysis of 30000 compounds

A quick and simple tool for validating of crystal structure

Sale, M. & Avdeev, M. (2012). J. Appl. Cryst. 45, 1054–1056

Brown, I. D. (2009). Chem. Rev. 109, 6858–6919

Na_xCoO_2

O3

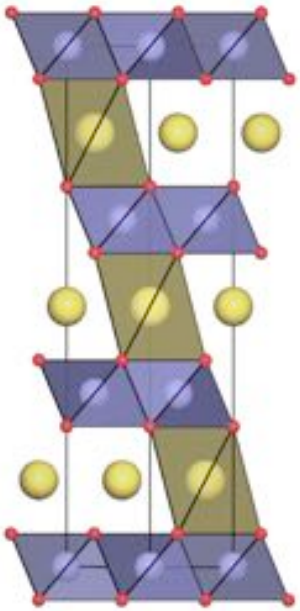

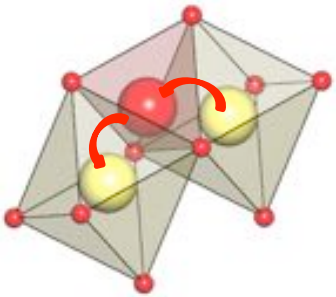

Emin -3.2 eV

Eact 3.8 eV

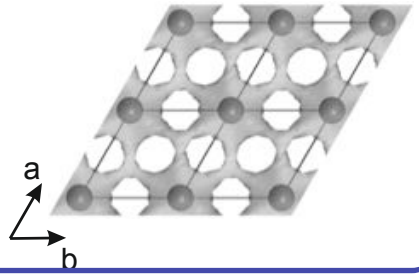

+/-0.6 b. u.

P2

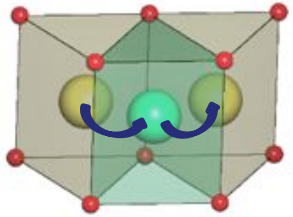

Emin -3.3 eV

Eact 0.9 eV

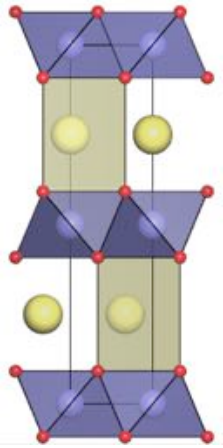

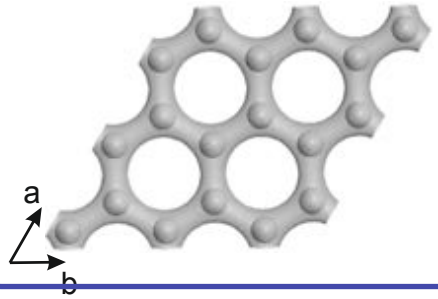

+/-0.3 b. u.

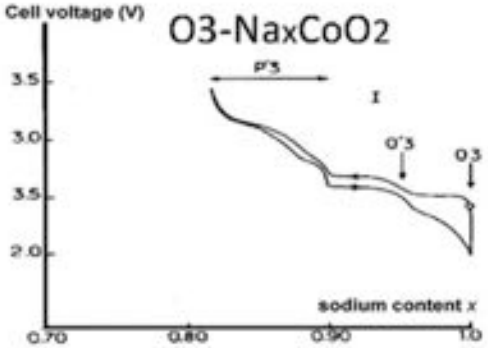

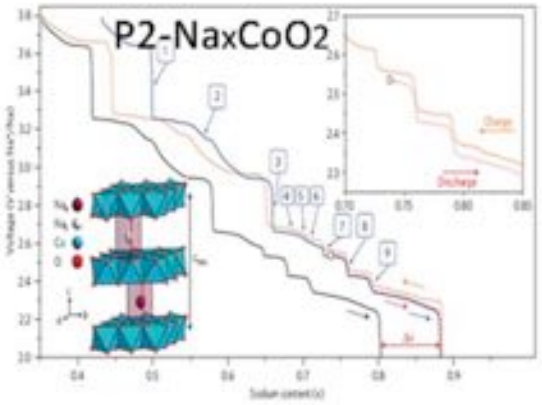

Search for new cathode materials

ionicity of the M - L bond

inductive effect: $LiFePO_4$ (J. Goodenough 1997)*

compounds with polyanions $(XO_m)^{n-}$: $(BO_3)^{3-}$, $(SiO_4)^{4-}$, $(PO_4)^{3-}$, $(SO_4)^{2-}$

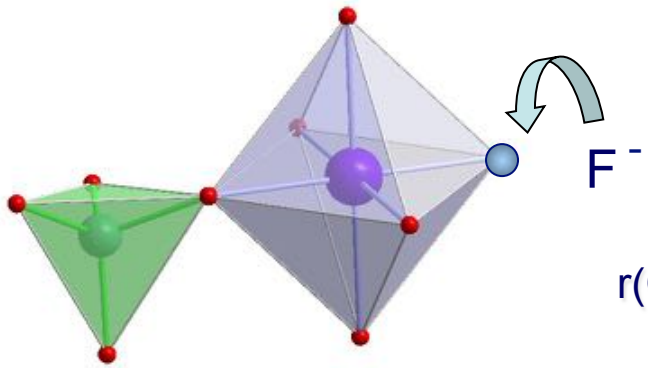

$r(O^{2-}) = 1.21Å \approx r(F^{-}) = 1.15Å$

inductive effect + higher ionicity of the M-F bond → high energy density

difference in formal charges → faster Li^+ transport → high power density

* A.K. Padhi et al. , *J. Electrochem. Soc.* 144 (1997) 1188

Search for new cathode materials

ionicity of the M - L bond

inductive effect: $LiFePO_4$ (J. Goodenough 1997)*

compounds with polyanions $(XO_m)^{n-}$: $(BO_3)^{3-}$, $(SiO_4)^{4-}$, $(PO_4)^{3-}$, $(SO_4)^{2-}$

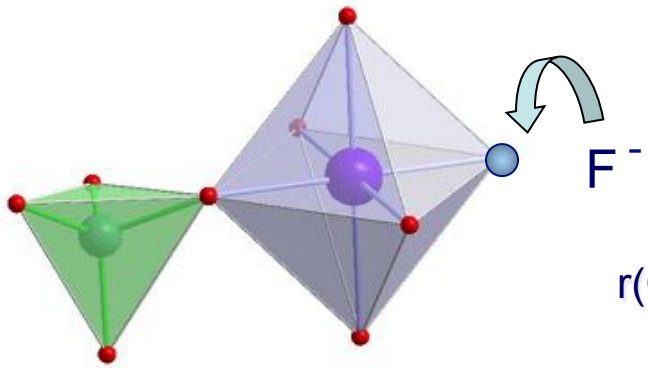

$r(O^{2-}) = 1.21Å \approx r(F^{-}) = 1.15Å$

inductive effect + higher ionicity of the M-F bond → high energy density

difference in formal charges → faster Li^+ transport → high power density

Compounds with two anions: $(XO_m)^{n-}$ and F^-

$(SO_4)^{2-}$ and F^-

$LiMSO_4F$**

$(PO_4)^{3-}$ and F^-

$LiMPO_4F$, **Li_2MPO_4F**

* A.K. Padhi et al. , *J. Electrochem. Soc.* 144 (1997) 1188

** G. Rousse and J.M. Tarascon, *Chem. Mat.* 26 (2014) 394

Fluoride-sulphates: $LiFeSO_4F$

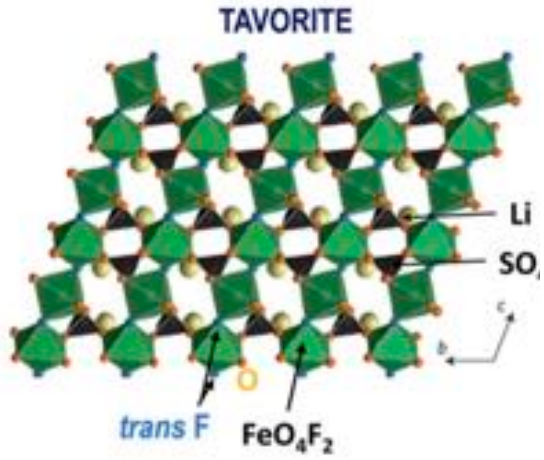

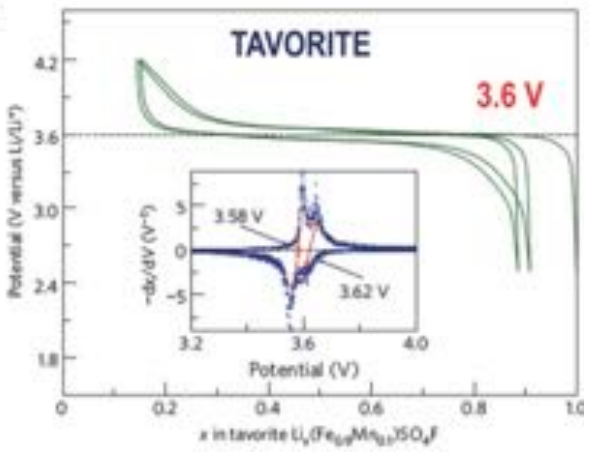

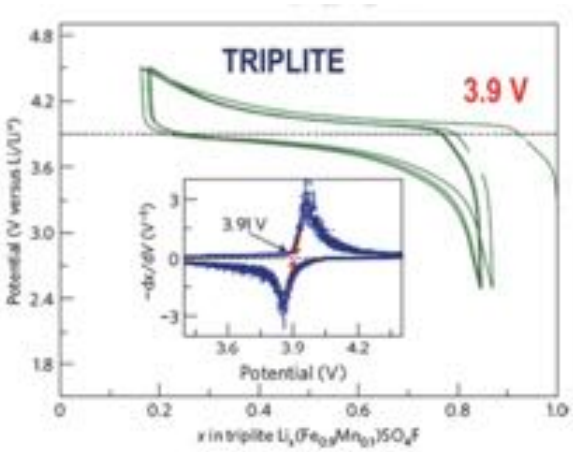

$FeSO_4 * H_2O + LiF \xrightarrow[300°C,\ IL]{} LiFeSO_4F + H_2O$

tavorite

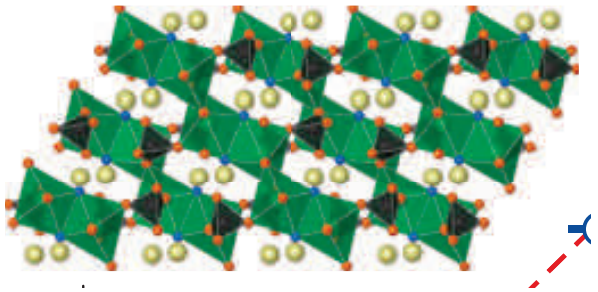

$LiMn_{0.05}Fe_{0.95}SO_4F$ - triplite

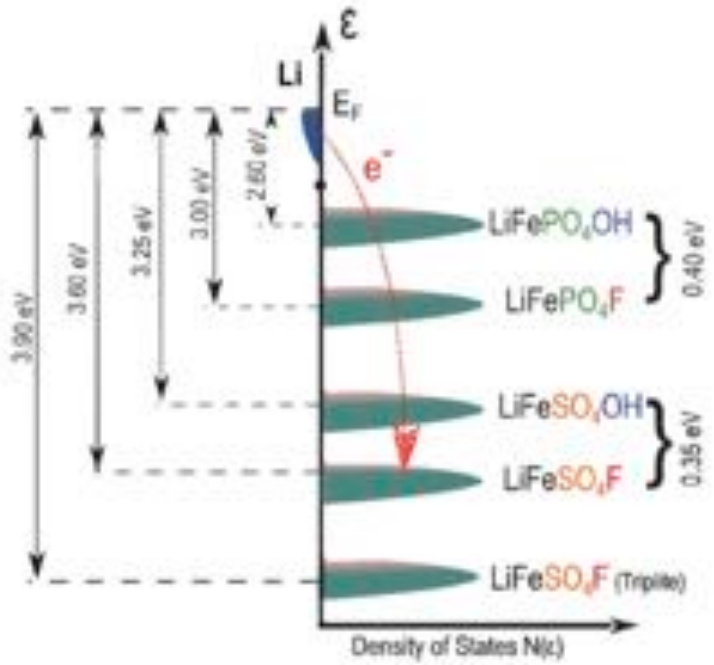

N. Recham et al, Nature Mater.9 (2010) 68

P. Barpanda et al, Nature Mater. 10 (2011) 772

Fluoride-phosphates A_2MPO_4F

- different conjugation of (MO_4F_2) octahedra
- different transition metal

$(NaLi)_2FePO_4F$ – 2D [1]

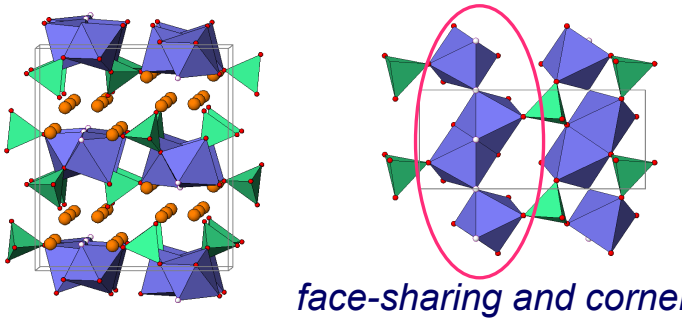

face-sharing and corner-sharing

Na_2MnPO_4F – 3D [2]

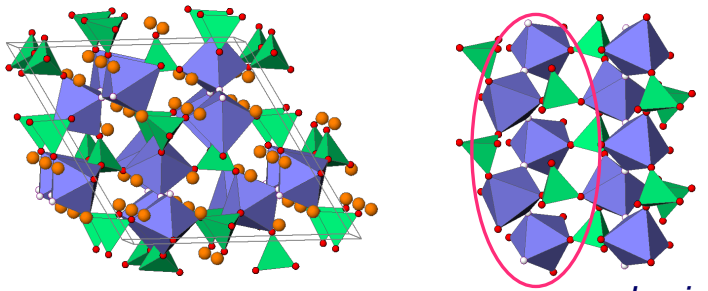

corner-sharing

Li_2MPO_4F (M=Ni, Co) – 3D [3,4]

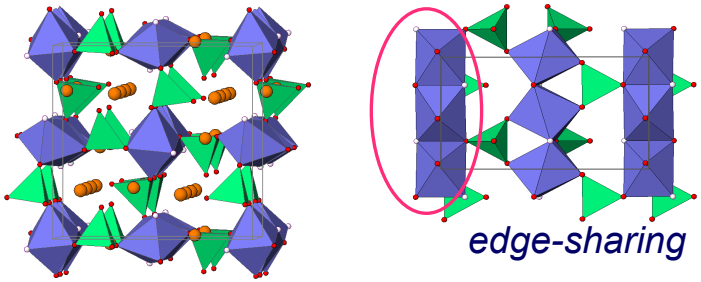

edge-sharing

C_T ~ 140 mAh/g for M^{2+}/M^{3+}

C_T ~ 280 mAh/g for M^{2+}/M^{4+}

1. B.L.Ellis *et al.*, *Nature Mat.* 6 (2007) 749
2. O.V.Yakubovitch *et al.*, *Acta Crystallogr.C* 53 (1997) 395
3. M. Dutreilh *et al.*, *JSSC* 142 (1999) 1
4. S. Okada *et al.*, *J. Power Sources* 146 (2005) 565

Crystal structure of Li_2CoPO_4F by Precession Electron Diffraction

Vainshtein, B.K. (1964) Structure analysis by electron diffraction. New York: Pergamon Press

326 intensities (≈ IFI^2) for structure determination were taken from 13 different zones

Co and P were found by direct methods (SIR2008), O(F) and Li from Fourier maps

Structure was refined by JANA 2006 (PO4 was used as rigid body)

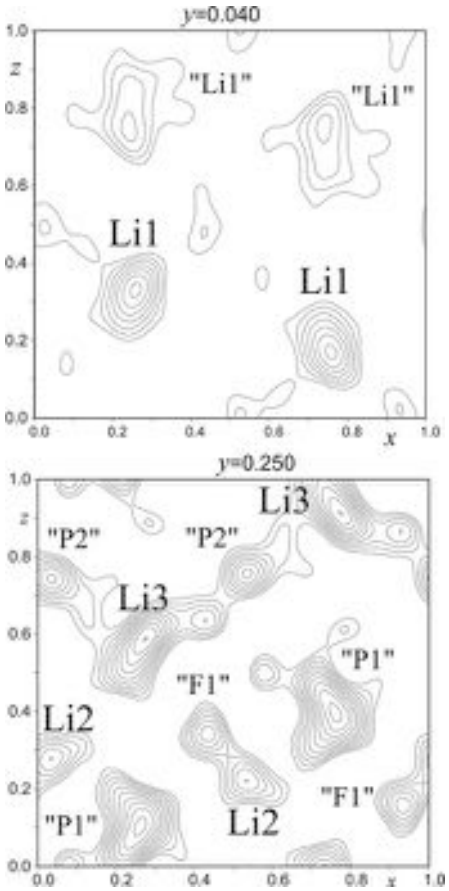

Difference Fourier maps

Detectability of light atoms (Vainstetn):

$$w = \left(\frac{Z_{light}}{Z_{heavy}} \right)^{\alpha}$$

XRD: α = 1.25 ED: α = 0.7

The Li positions are 3 times more "visible" in Li_2CoPO_4F with PED than with XRD!

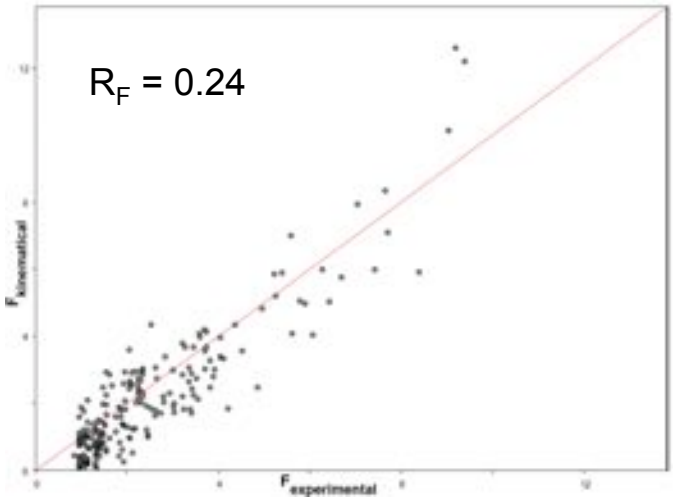

PED

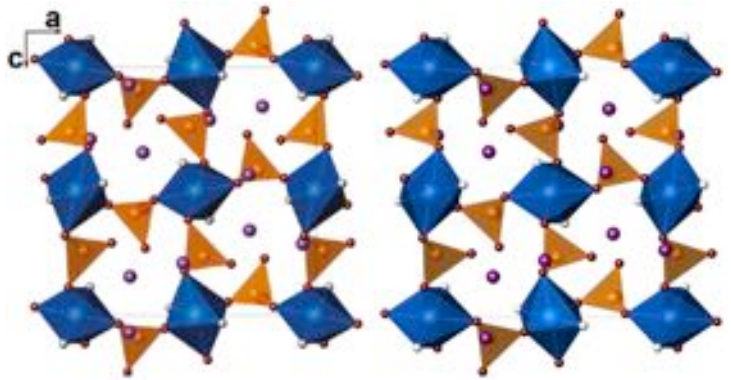

SXPD

J. Hadermann et al. , Chem. Mat. 23 (2011) 3540

3D-Li_2CoPO_4F: crystal structure

S.G.: Pnma

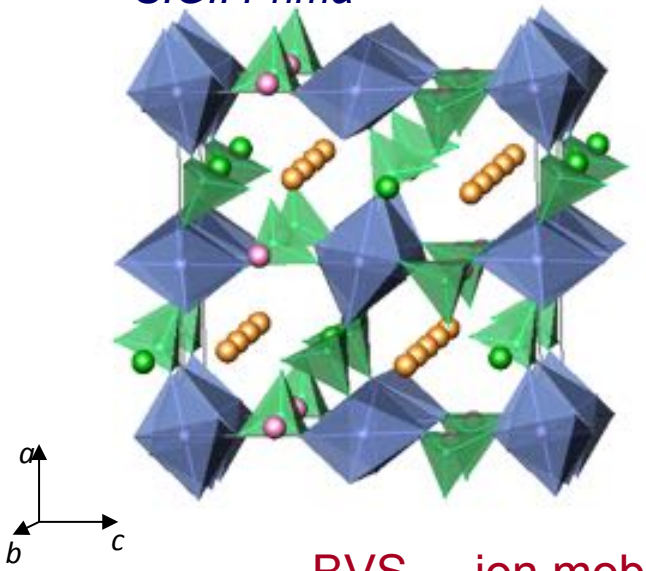

BVS mapping

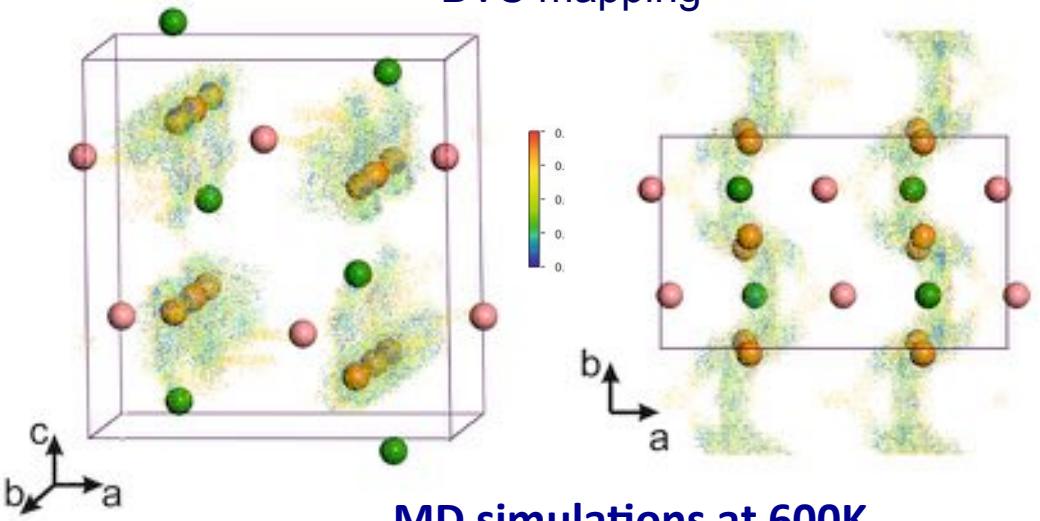

	BVS	ion mobility
- Li1 (*8d*)	+0.77	+
- Li2 (*4c*)	+0.98	?
- Li3 (*4c*)	+1.22	-

- 3D structure (thermal and electrochemical stability)
- 1D Li-ion diffusion pathway
- 3 independent Li-positions,
  Li-ion mobility: Li1 > Li2 > Li3

MD simulations at 600K

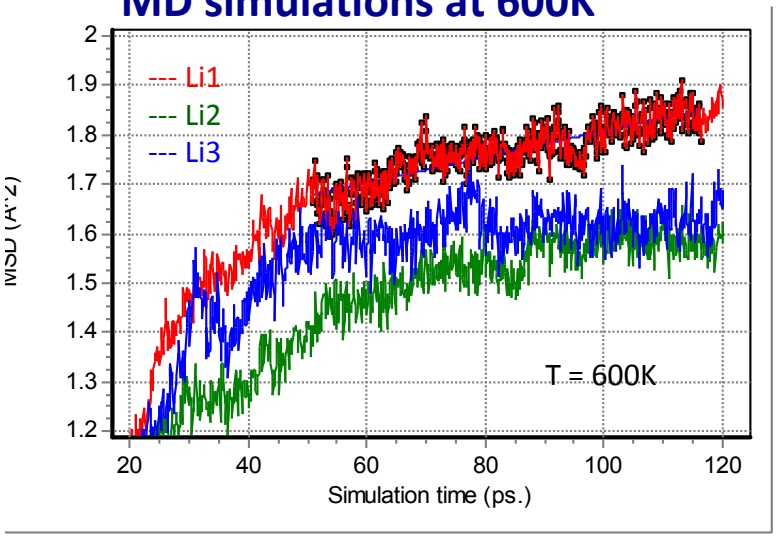

D(Li3)~0 (plateau is reached)

D(Li2) = $9.5*10^{-8}$ cm^2/s

D(Li1) = $3.3*10^{-7}$ cm^2/s

Li_2CoPO_4F: electrochemical measurements

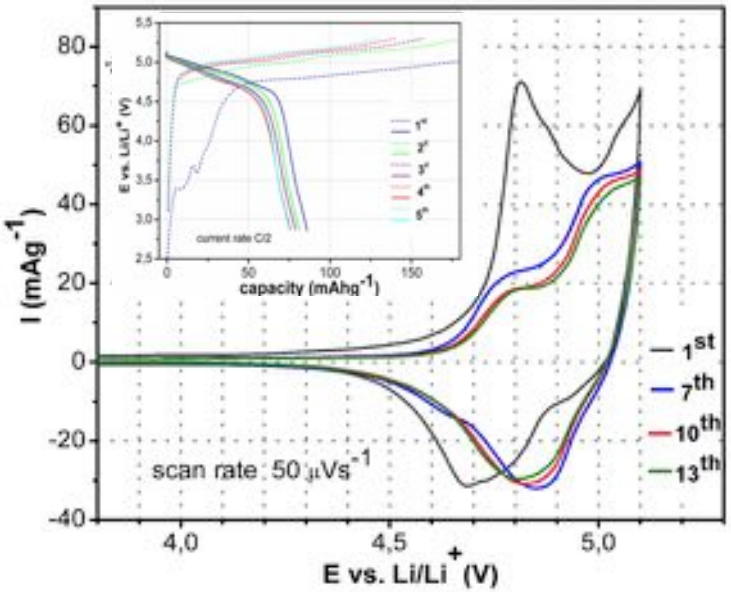

CV in the potential range 3.0-5.1 V at the scan rate 50 μVs-1. The insert- charge-discharge performance at C/2 cycling rate.

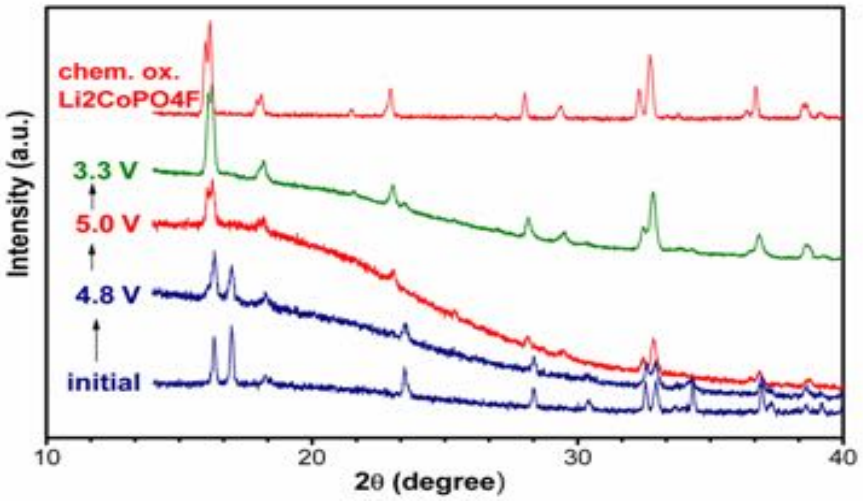

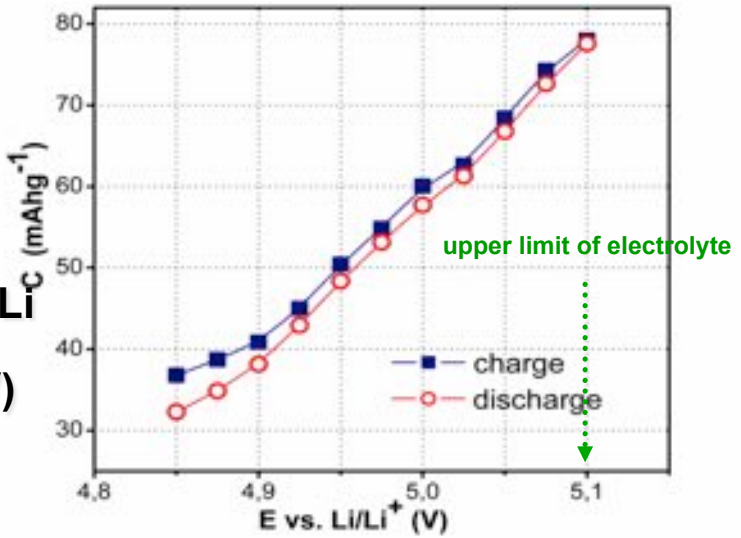

Capacity vs. voltage: from potentiostatic step measurements (4.2 V and variable anodic potentials)

- discharged capacity of 80 mAh/g ~ 0.55 mole Li
- slope : ~ 0.7 V per 1Li mole (x=1 at about 5.5 V)
- "solid solution" behavior
- structure transformation at >4.8 V

Li_2CoPO_4F: structure transformation upon Li-extraction

Li_2CoPO_4F

a =10.45452(8) Å
b = 6.38525(5) Å
c = 10.87550(9) Å
V=725.99(1) Å^3

oxidation (- Li^+)

$Li_{1.3}CoPO_4F$

a = 10.94923(9) Å
b = 6.28318(8) Å
c = 11.0680(11) Å
V=760.43(1) Å^3

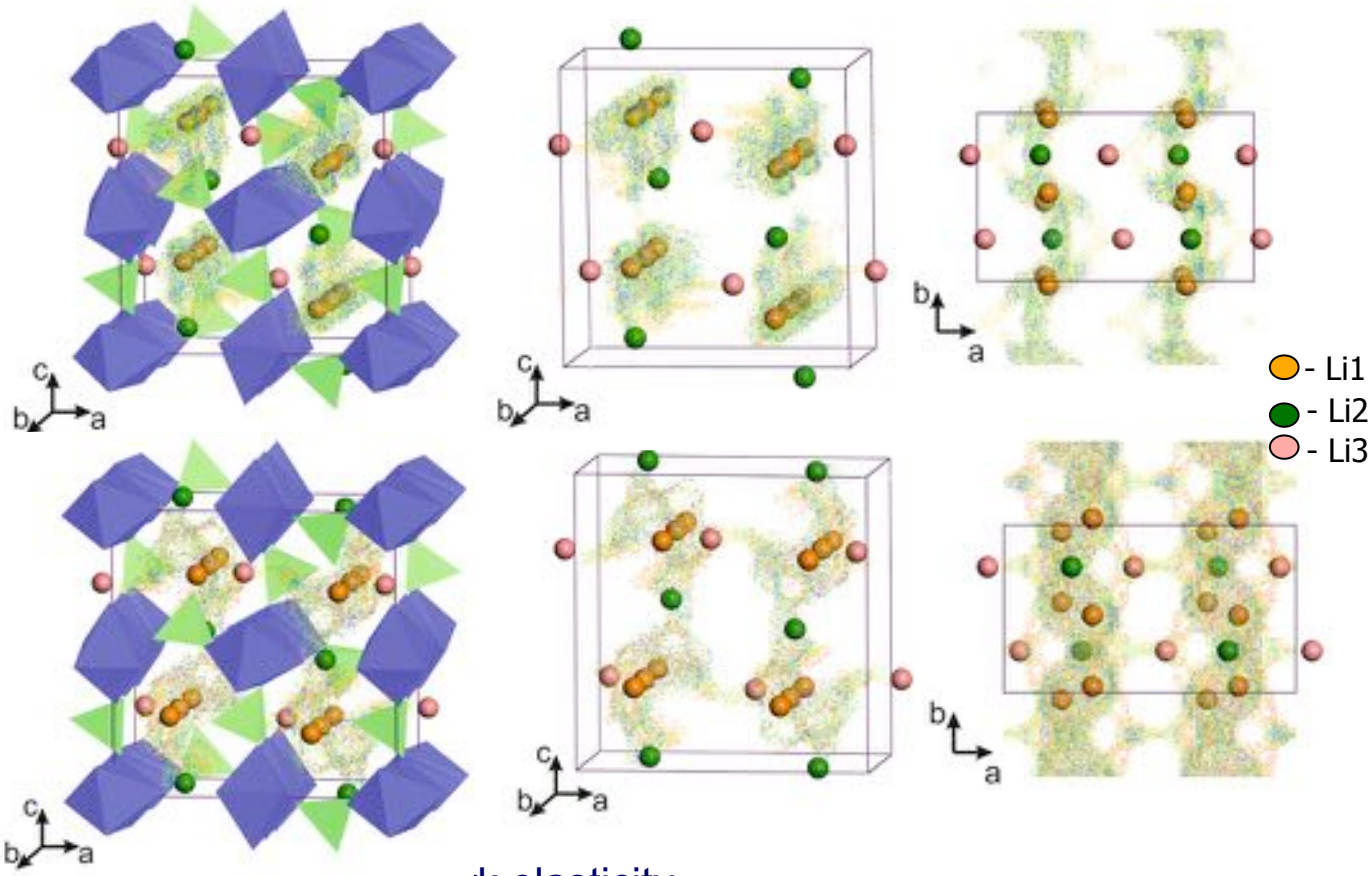

- volume expansion of Δ V ~ 5% → framework elasticity
- enlarging of diffusion channels
- involving of Li2 in diffusion : extraction of 1.5 Li^+ per f.u. ??? **at 5.9 V (?)**
- unit cell expansion favors Li^+-ion diffusion in the modified framework
- **"fine structure tuning "**

to decrease the working potential !

N.R. Khasanova et al., J. of Power Sources 196 (2011) 355

$Li_2(Co_{1-x}M_x)PO_4F$ with M=Fe, Mn

M	Mn^{2+}	Fe^{2+}	Co^{2+}	Ni^{2+}
r, Å	0.83	0.78	0.74	0.69
E* (M^{2+}/M^{3+}), V	4.1	3.45	> 4.8	>5.2

* for olivine-type materials

- **narrow range of solid solutions:**

$Li_2(Co_{1-x}Fe_x)PO_4F$ $x \leq 0.3$

$Li_2(Co_{1-x}Mn_x)PO_4F$ $x \leq 0.1$

"framework elasticity": **Li^+ → Na^+**

0.76 Å → 1.02 Å

N.R. Khasanova et al., Beilshtein J. Nanotech. 4 (2013) 860

$NaLiFePO_4F$: preparation and characterization

Synthesis: $LiFePO_4(C) + NaF \xrightarrow[\text{Ar-flow}]{\sim 650\text{-}670^\circ C} NaLiFePO_4F(C)$

ICP analysis: $Na_{1.01}/Li_{1.05}/Fe_{0.97}/P_{1.00}$

X-ray diffraction

	a, Å	b, Å	c, Å	V, Å^3
$NaLiFePO_4F$	10.977 (2)	6.3627(11)	11.429 (2)	798.6(3)
Li_2CoPO_4F	10.4578(13)	6.3887(5)	10.877(2)	726.1(2)

Rietveld refinement

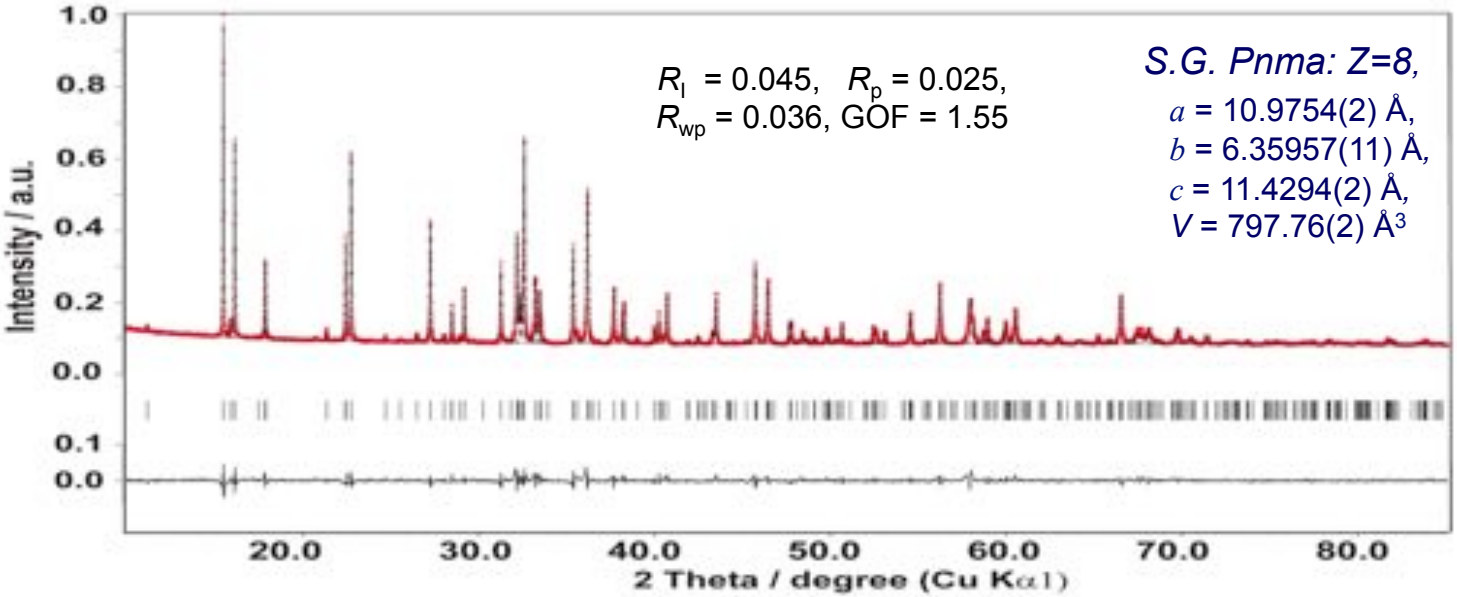

Electron diffraction

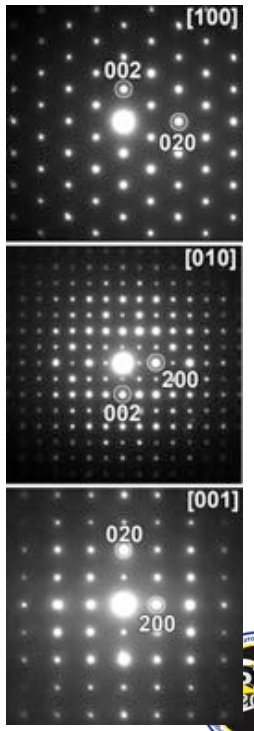

H.Mizuta, ECS Fall Meeting, 2011, Abstract No. 404.
N.R. Khasanova et al., J. Chem. Mat. 24 (2012), 4271.
H. B. Yahia et al. Dalton Trans. 41 (2012), 11692.

$NaLiFePO_4F$: structure and properties

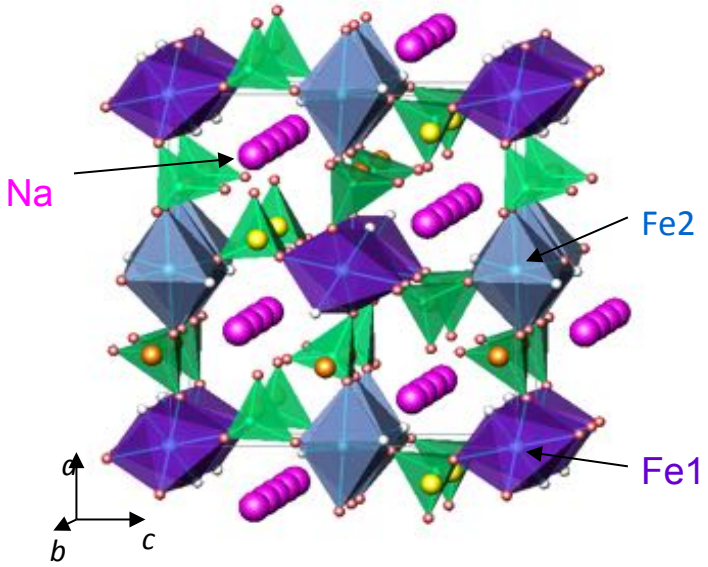

• Mössbauer spectroscopy

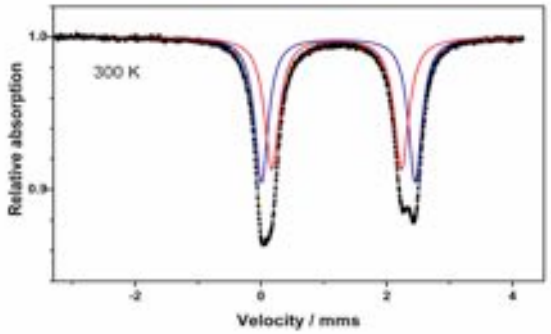

- **complete ordering of Na^+ and Li^+ ions**
- **Fe^{2+} on the two octahedral sites**

• Electrochemical performance

Li-cell, 1M $LiPF_6$ in EC/DMC

- **reversible deintercalation with discharge capacity of ~110 $mAhg^{-1}$**

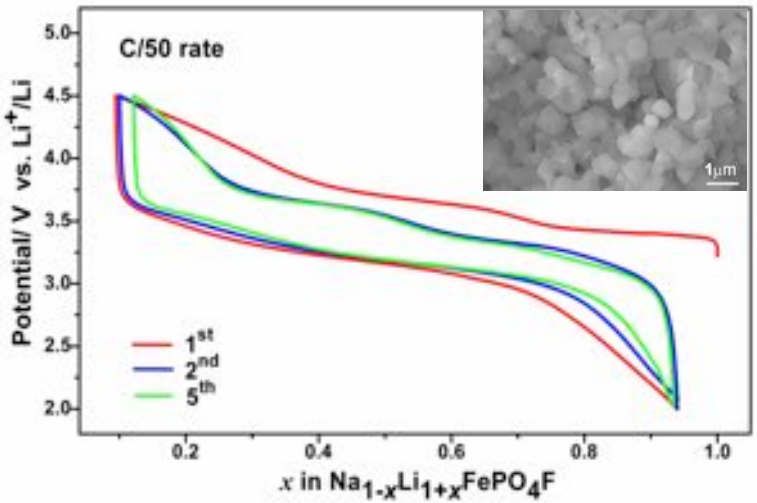

$NaLiFePO_4F$: *ex-situ* investigation

XRD pattern

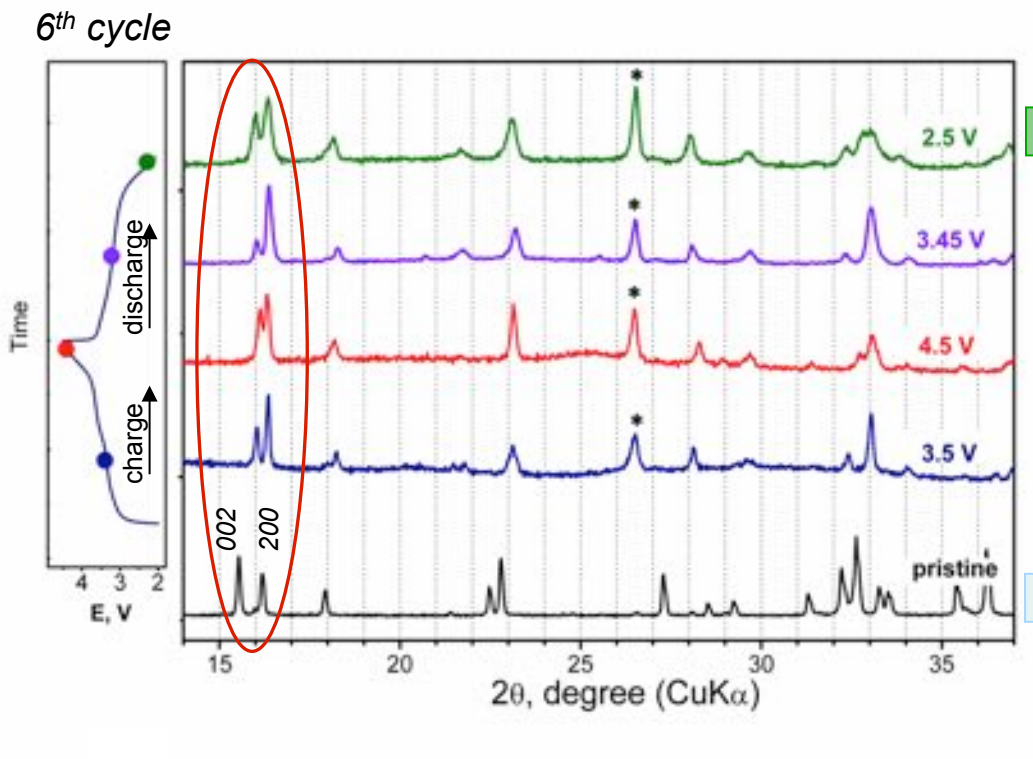

Simulation

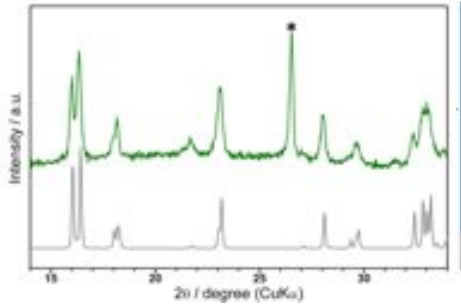

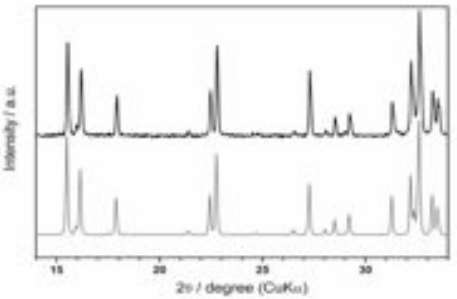

EDX

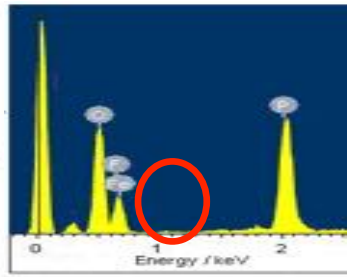

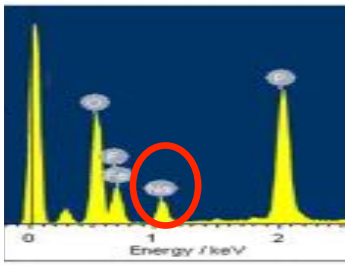

- shift of peaks
- redistribution of intensities for *002* and *200* peaks
- EDX data

3D- Li_2FePO_4F

a = 10.775(5)Å
b = 6.266(4) Å
c = 11.027(6) Å
V = 744.5(6) Å^3

- continuous shift of peaks → solid solution behavior
- volume change between charged and discharged states of 1.7%

Li_2FePO_4F: electrochemical performance

Li-cell, 1M $LiPF_6$ in EC/DMC

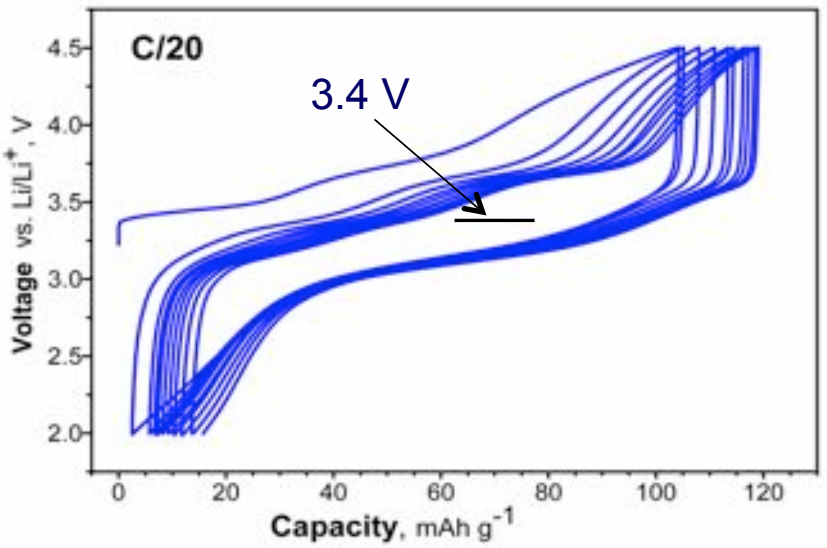

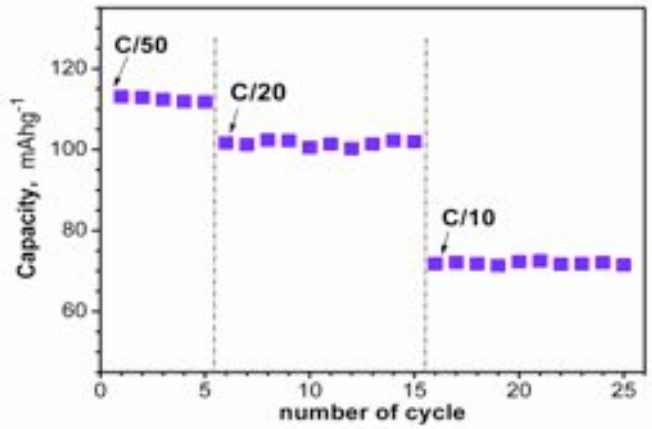

- PITT: 2.7-3.7-2.7 V (vs. Li/Li^+), 0.05 V step

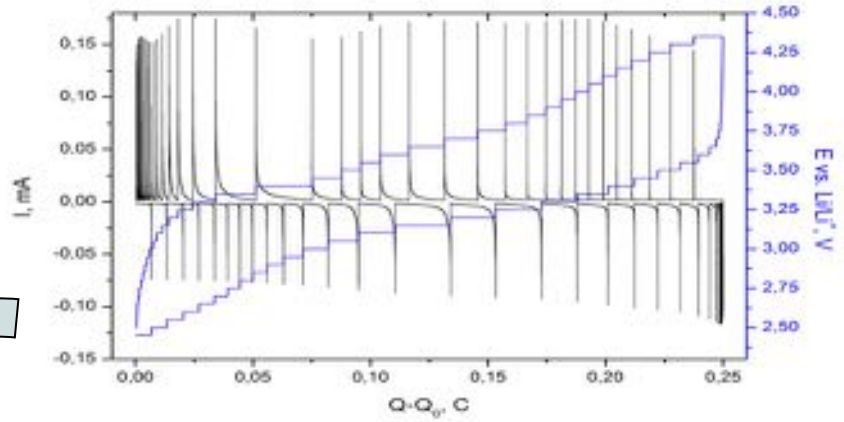

- discharge capacity ~114 mAh/g (0.84 Li)
- working potential ~ 3.4 V
- stable cycling
- "solid solution" de/intercalation mechanism (no interfacial problems)

$D \sim 10^{-11}$ cm^2/s

$LiCoO_2$: $D \sim 10^{-9}$ cm^2/s $LiFePO_4$: $D \sim 10^{-15}$ cm^2/s

N.R. Khasanova et al., Chem. Mat. 24 (2012) 4271

Concluding remarks: Li_2MPO_4F vs. $LiFePO_4$

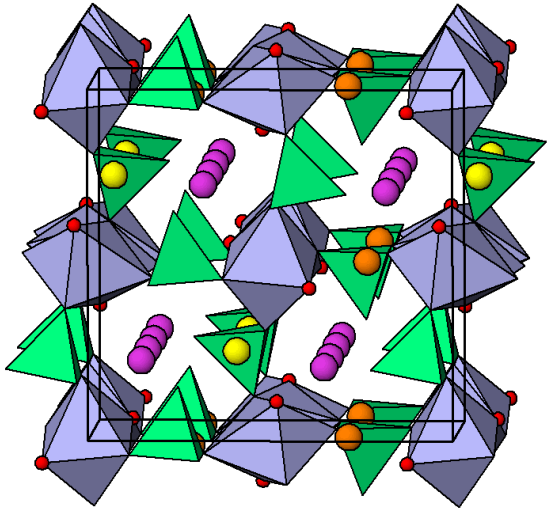

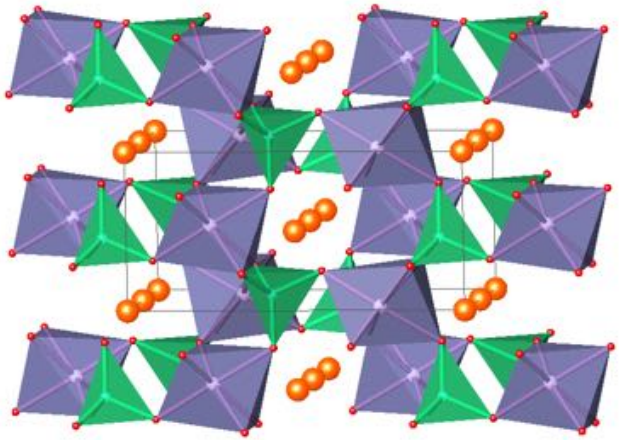

	solid solution	2-phase mechanism
D_{chem}	≈ 10^{-10} cm^2/s	≈ 10^{-15} cm^2/s

	Co	Fe	
Volume change (%)	~ 4.5 %	1.7%	6.7%
E_g for 1Li (Wh/kg)	**730**	496	583
E_g for 1.5 Li (Wh/kg)	**1095**	**744**	-

Perspectives of Fluoride-phosphates as cathodes for LIB

Chemical composition	Dimensionality of polyhedra network / Li-ion diffusion pathway	Average potential vs. Li^+/Li^0 (V)	Theoretical specific capacity (mAh/g)/ energy (Wh/kg)*
$LiFePO_4$	3D / 1D	3.43	170 / 583
$LiVPO_4F$	3D/ 1D	4.2	156 / 655
Li_2VPO_4F	3D/ 1D	1.8	150 / 270
Li_2FePO_4F (tavorite type)	3D/ 1D	2.9	146 / 423
Li_2FePO_4F (layered type)	2D / 2D	3.3	146 / 482
Li_2FePO_4F (3D type)	3D / 1-2D	3.4	146 / 496
Li_2MnPO_4F	3D / 2D	3.9	147 / 573
Li_2CoPO_4F	3D / 1-2D	5.1	143 / 730

J. Barker et al., Electrochem. Solid-State Lett. 6 (2003); B.L. Ellis et al., Nature Mat. 6 (2007); N. Recham et al., Chem. Mater. 22 (2010) 1142.

E.V. Antipov et al., IUCr Journal 2 (2015) 85-94

Acknowledgements

Department of Chemistry, Moscow State University

Oleg Drozhzhin
Stanislav Fedotov
Nellie Khasanova
Darja Storozhilova
Dmitry Filimonov

ICMCB, Bordeaux

Claude Delmas

FLNP, JINR, Dubna

EMAT, RUCA, Antwerp

Artem Abakumov
Joke Hadermann

A.M. Balagurov
I.A. Bobrikov

Funding from RFBR and SkolTech